# Hybrid Sulfur flowsheets using PEM electrolysis and a bayonet decomposition reactor

Maximilian B. Gorensek[*], William A. Summers

*Savannah River National Laboratory, Aiken, SC 29808  USA*

## Abstract

A conceptual design is presented for a Hybrid Sulfur process for the production of hydrogen using a high-temperature nuclear heat source to split water.  The process combines proton exchange membrane-based $SO_2$-depolarized electrolyzer technology being developed at Savannah River National Laboratory with silicon carbide bayonet decomposition reactor technology being developed at Sandia National Laboratories.  Both are part of the US DOE Nuclear Hydrogen Initiative.  The flowsheet otherwise uses only proven chemical process components.  Electrolyzer product is concentrated from 50 wt% sulfuric acid to 75 wt% via recuperative vacuum distillation.  Pinch analysis is used to predict the high-temperature heat requirement for sulfuric acid decomposition.  An Aspen Plus™ model of the flowsheet indicates 340.3 kJ high-temperature heat, 75.5 kJ low-temperature heat, 1.31 kJ low-pressure steam, and 120.9 kJ electric power are consumed per mole of $H_2$ product, giving an LHV efficiency of 35.3% (41.7% HHV efficiency) if electric power is available at a conversion efficiency of 45%.

[*] Corresponding author. Tel.: (803) 725-1314; Fax: (803) 725-8829;
E-mail address: maximilian.gorensek@srnl.doe.gov

# 1.     Introduction

The push for a Hydrogen Economy in the United States (U.S.) is largely driven by the desire to replace fossil-based, hydrocarbon fuels for transportation, particularly in automobiles. Fuel cell-powered vehicles fueled with hydrogen ($H_2$) emit no greenhouse gases – only water – and their fuel can be derived from greenhouse gas-neutral, non-fossil energy sources.  If the U.S. should transition to a Hydrogen Economy, the National Academies have projected that the $H_2$ needed to fuel all U.S. light-duty vehicles alone will reach 110 MMt/yr by 2050 [1].  This has a power equivalent of 450 $GW_{th}$ and represents a twelve-fold increase over current U.S. $H_2$ consumption, which is primarily for industrial needs.  For comparison, the average U.S. electric power demand in 2007 was 446 $GW_e$ [2].  Other uses for $H_2$ (heavy-duty vehicles, fertilizer and chemicals manufacturing, distributed power, etc.) could easily double the total demand over that for light-duty vehicles.  The energy required to make so much $H_2$ would be comparable to that needed for electric power generation.  As a result, it will necessarily rely on multiple primary energy sources, such as fossil fuels (with carbon dioxide sequestration), renewable energy coupled with electrolysis, and nuclear water-splitting, in much the same way that the U.S. electricity supply does currently.

The U.S. Department of Energy's Office of Nuclear Energy, Science & Technology (DOE-NE) has established the Nuclear Hydrogen Initiative (NHI) to develop technologies that can be coupled with next generation nuclear reactors to produce $H_2$ on such a massive scale. Thermochemical water-splitting cycles are leading contenders within the NHI program because they have the potential for higher efficiencies than water electrolysis with more favorable scale-up characteristics.

Research programs world-wide recognize sulfur-based thermochemical cycles as high priority candidates for research and development. The NHI has identified the Hybrid Sulfur (HyS) and the Sulfur-Iodine (SI) cycles as the two first priority baseline cycles. Both have the potential for significantly higher thermal efficiency than water electrolysis, and both have been demonstrated at the laboratory scale to confirm performance characteristics. The two cycles share a common, high-temperature reaction step – the catalytic, vapor phase thermal decomposition of sulfuric acid ($H_2SO_4$).

The Savannah River National Laboratory (SRNL) has been tasked by the NHI with developing the $SO_2$-depolarized electrolyzer (SDE), which distinguishes the HyS from other sulfur cycles. As part of this work, SRNL has also prepared conceptual designs of HyS processes that use SDEs of the type being developed and that are powered by an advanced nuclear reactor heat source. The purpose of this manuscript is to communicate the results of the latter task to date.

## 2. Background

### 2.1 The Hybrid Sulfur cycle

The HyS cycle was first proposed by Brecher and Wu [3] at Westinghouse Electric Corp., where it was extensively developed in the 1970s and 1980s [4,5,6]. As a result, it has also come to be known as the Westinghouse process [7]. HyS is one of the simplest thermochemical cycles, comprising only two reaction steps and having only fluid reactants. The "hybrid" designation acknowledges the electrochemical nature of one of the reaction steps, which requires that electric as well as thermal energy be supplied to the process. It is a sulfur cycle because it

entails sulfur oxidation and reduction. In fact, sulfur is the only element in the cycle other than

$H_2$ and oxygen ($O_2$).

A simple schematic of the HyS cycle that illustrates the two reaction steps and how they

interact to split water is shown in Fig. 1. The first reaction step,

$$H_2SO_4(aq) \rightarrow H_2O(g) + SO_2(g) + \tfrac{1}{2}O_2(g) \tag{1}$$
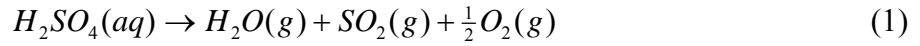
common to all sulfur cycles, is, in reality, the result of two separate reactions. As $H_2SO_4$ is

vaporized and superheated, it spontaneously decomposes into water ($H_2O$) and sulfur trioxide

($SO_3$),

$$H_2SO_4(aq) \rightarrow H_2O(g) + SO_3(g). \tag{1a}$$
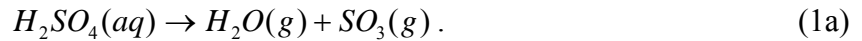
Further heating the vapor to high temperatures (>800 °C, 1073 K) in the presence of a catalyst

drives the endothermic decomposition of $SO_3$ into $O_2$ and sulfur dioxide ($SO_2$),

$$SO_3(g) \rightarrow SO_2(g) + \tfrac{1}{2}O_2(g) \tag{1b}$$

After $O_2$ is removed as a co-product, the $SO_2$ and $H_2O$ are combined with make-up $H_2O$ (and

recycled $H_2SO_4$) and fed to the anode of an electrolyzer, where the second reaction takes place.

This is the $SO_2$-depolarized electrolysis of water,

$$SO_2(aq) + 2H_2O(l) \rightarrow H_2SO_4(aq) + H_2(g) \tag{2}$$
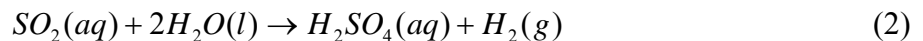
illustrated in Fig. 2. $SO_2$ is electrochemically oxidized at the anode to form $H_2SO_4$, protons and

electrons.

$$SO_2(aq) + 2H_2O(l) \rightarrow H_2SO_4(aq) + 2H^+ + 2e^- \tag{2a}$$
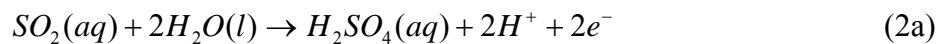
The protons are conducted across the electrolyte separator to the cathode, where they recombine

with the electrons, which pass through an external circuit, to form $H_2$.

$$2H^+ + 2e^- \rightarrow H_2(g) \tag{2b}$$

The net result is $H_2SO_4$ production at the anode and $H_2$ production at the cathode. $H_2SO_4$ is recycled to the high-temperature decomposition step to complete the cycle, while $H_2$ is removed as the principal product.

What makes the HyS cycle attractive is the standard cell potential for $SO_2$-depolarized electrolysis, which is only -0.158 V at 25 ºC (298 K) in water [8,9]. The reversible potential increases in magnitude to -0.243 V if $SO_2$ is dissolved to saturation at 1 bar total pressure in a 50-wt% $H_2SO_4$-$H_2O$ solution, the most likely anolyte[1]. This means that the SDE will consume much less electricity per mole of $H_2$ product than water electrolysis, which has a reversible cell potential of -1.229 V at 25 °C (298 K) [8,9], and which is an obvious $H_2$ production alternative.

In reality, water electrolyzers operate at cell potentials of -1.7 to -2.0 V when economically reasonable current densities are maintained. Ohmic losses and electrode overpotentials are responsible for this voltage increase. Likewise, SDEs in which the $SO_2$ is dissolved in 50 wt% $H_2SO_4$ are expected to operate with cell potentials significantly greater than -0.243 V at practical current densities.

In 1981, Lu et al. [10] predicted that cell potentials of -0.45 to -0.75 V could be obtained at current densities of 100 to 400 $mA/cm^2$ for properly designed and optimized SDEs. Recent experience with proton exchange membrane (PEM) SDE development at SRNL suggests that cell potentials of -0.6 V should be attainable at practical current densities with higher operating temperatures ($\geq$100 °C, 373 K) and pressures ($\geq$10 bar). The target of SRNL's SDE development program is, in fact, a potential of -0.6 V at a current density of 500 $mA/cm^2$.

Therefore, it is anticipated that the HyS SDE will operate with a cell potential significantly lower than that of a conventional alkaline electrolyzer.

---

[1] Correction for nonstandard condition calculated using the Nernst equation [9], with species activities obtained from the Mixed Solvent Electrolyte model in OLI Systems, Inc.'s OLI Engine 7.0.

## *2.2     Energy considerations*

A key benchmark against which the HyS cycle will ultimately be judged is the use of conventional nuclear power generation coupled with water electrolysis.  Both are proven technologies that could be deployed almost immediately, although this would require a large scale-up from existing water electrolysis plants.  In order for the more complex HyS cycle to be competitive with the simpler, direct electrolysis of water, it needs to provide a significant advantage in terms of higher process thermal efficiency.  No capital cost estimates were included in this study, but some general observations can be made about the competing hydrogen production options.

If the HyS plant has a higher thermal efficiency, it will require a smaller nuclear heat source than the water electrolyzer plant.  Since the nuclear heat source is expected to be the most capital intensive portion of the plant, the nuclear-HyS plant could be expected to have a lower total capital investment (nuclear plant plus hydrogen plant) and a resulting lower hydrogen production cost.  This could be offset, however, if there is an overwhelming difference in the capital cost between the two hydrogen production processes, or if the efficiency difference is minor.  Further studies will investigate this issue and the trade-offs between plant efficiency and capital cost.  Qualitatively, however, it is clear that the HyS plant efficiency must be substantially better than the water electrolysis plant efficiency.

Existing nuclear power plants generate electricity using either a boiling water reactor (BWR) or pressurized water reactor (PWR) combined with a steam-driven Rankine cycle power conversion unit (PCU).  The maximum temperature of the steam is typically less than 315 °C (588 K), and the overall thermal-to-electric conversion efficiency for the power plant is

approximately 33%. $H_2$ can be produced via water electrolysis with an electric-to-lower heating value (LHV) conversion efficiency of 62 to 68% [11,12] [2]. Combining the two steps would allow $H_2$ to be produced from nuclear energy at an overall LHV efficiency of 21 to 23%. This represents a heat requirement of 4.5 $MW_{th}$ of fission heat to make a one-$MW_{th}$ equivalent of $H_2$ (in terms of fuel value) using conventional nuclear power plant (BWR or PWR) technology.

The overall efficiency could be increased by utilizing an advanced Generation IV nuclear reactor system, such as the high-temperature gas-cooled reactor (HTGR), which has a higher thermal-to-electric conversion efficiency. An HTGR can produce hot helium at 850 to 950 °C (1123 to 1223 K) and be combined with a helium-driven closed-loop Brayton cycle PCU. The resulting thermal-to-electric conversion efficiency could be between 42% and 48%, depending on the exact cycle design. In that case, the overall LHV efficiency of $H_2$ production for an HTGR-water electrolysis hydrogen plant could be as high as 33%, or 3.0 $MW_{th}$ of fission heat per one-$MW_{th}$ equivalent of $H_2$.

The HyS plant will require both electricity for the SDE and thermal energy for acid decomposition. In order for the HyS plant to exceed the nuclear-electrolysis plant efficiency, the thermal energy required to effect the decomposition of $H_2SO_4$ will need to be substantially less than the thermal equivalent of the difference in cell potentials between the SDE and the water electrolyzer. The electric power requirement for the HyS electrolysis step is 116 kJ/mol $H_2$ product, based on an assumed SDE cell potential of -0.6 V. If a conventional BWR/PWR nuclear reactor is used to produce this electricity, the thermal equivalent is 352 kJ/mol $H_2$. On the other hand, if an HTGR power plant operating with an assumed thermal-to-electric

---

[2] Alkaline electrolysis can produce $H_2$ at pressure using 4.8 kWh/$Nm^3$ [11], while PEM electrolysis requires about 4.4 kWh/$Nm^3$ [12]. These figures are equivalent to 387 and 355 $kJ_e$/mol $H_2$, respectively. The LHV, or lower heating value, of $H_2$ is 242 kJ/mol. An LHV efficiency of 68% implies that 242/0.68 = 356 kJ of electric energy is needed to make 1 mol $H_2$. For comparison, the HHV, or higher heating value, of $H_2$ is 286 kJ/mol, so an $H_2$ LHV efficiency of 68% is equivalent to an $H_2$ HHV efficiency of 80.3%.

conversion efficiency of 45% is used instead, the thermal equivalent of the power for the SDE is only 258 kJ/mol $H_2$.  Table 1 shows the calculation for "allowable" thermal energy use in the HyS plant compared to the water electrolysis plant.

BWR/PWR-powered water electrolysis at 22.4% overall LHV efficiency would consume 1,080 kJ of thermal energy per mol $H_2$ product.  That leaves an allowance of as much as 1,080 kJ – 352 kJ = 728 kJ heat per mol $H_2$ for the $H_2SO_4$ decomposition step for the HyS plant to achieve the same overall plant efficiency.  If a more efficient HTGR nuclear plant is used to generate the electricity, the HTGR-powered water electrolysis would have a 30.6% overall LHV efficiency and would only consume 791 kJ of thermal energy per mol $H_2$ product.  This would leave an allowance of 791 kJ – 258 kJ = 533 kJ heat per mol $H_2$ for the $H_2SO_4$ decomposition step. A reasonable goal for the HyS plant might be a high-temperature heat requirement for $H_2SO_4$ decomposition (and auxiliaries) of no more than about 450 kJ/mol $H_2$.  In that case, the HyS plant would be about 25% and 10% more efficient than a water electrolysis plant using conventional and advanced nuclear power plants for electricity production, respectively.

## 2.3    *The bayonet decomposition reactor*

One of the most difficult challenges in decomposing sulfuric acid at high temperatures (>800 °C, 1073 K) and pressures (up to 90 bar) is finding a material that can contain the process at the required conditions without significantly corroding or deteriorating, while providing adequate heat transfer characteristics.  Silicon carbide (SiC) is among the handful of substances identified so far that meet these requirements.  Since SiC is ceramic, it can not be shaped as easily as metal.  This greatly complicates the design and fabrication of process vessels and fluid

conduits.  A particular concern is making and maintaining sealed joints between individual SiC and SiC-metal components that operate at high temperature and pressure.

As noted above, the two leading thermochemical cycles share the high-temperature decomposition of sulfuric acid as a common step.  Responsibility for developing this reaction process for the NHI program belongs to Sandia National Laboratories (SNL), which was initially assigned to do this as part of an international collaboration with General Atomics (GA) and France's Commissariat à l'Energie Atomique (CEA) to build an integrated SI cycle demonstration at GA [13].  The same process should be easily adaptable to the HyS cycle, with minor modifications.

SNL has devised an innovative solution that makes use of readily available SiC shapes and does not have any high-temperature connections [14].  Their bayonet decomposition reactor features internal recuperation and allows all of the connections to be made at relatively low temperatures, where polytetrafluoroethylene (PTFE) and similar materials can be used for seals.  The essential elements of SNL's bayonet decomposition reactor are shown in Fig. 3.

In its simplest form, the reactor consists of one closed ended SiC tube co-axially aligned with an open ended SiC tube to form two concentric flow paths.  A baffle tube may be included to enhance heat transfer.  High-temperature heat is applied externally, except near the open end.  Concentrated liquid $H_2SO_4$ is fed at the open end to the annulus, where it is vaporized before passing through an annular catalyst bed.  The decomposition reaction takes place in the catalyst bed, using heat provided by the external heat source.  $SO_2$, $O_2$, and $H_2O$ vapor product returns through the center and loses its heat to the feed through recuperation.  Cooled and partially condensed product exits out the open end into a metal base or manifold at a temperature low

enough ($\leq$ ~250 °C, or 523 K) to allow the use of PTFE seals.  Imbedding the open ends of the

SiC tubes in a metallic manifold facilitates the transition to metal pipe.

The catalyst for this reactor is being developed by Idaho National Laboratory (INL) as

part of the NHI.  Metal oxide-supported platinum has been shown to have good activity, but

lacks long-term stability and is costly [15].  The focus of the INL work has recently shifted to

complex metal oxides, which look more promising [16].

Heat transfer limitations will impose a high surface-to-volume ratio limit, keeping

diameters small, so it should be obvious that a single bayonet will not have sufficient capacity

for a full-scale reactor. However, it is easy to envision an arrangement in which many bayonets

are attached in parallel to a manifolded base plate to achieve the necessary production rate.  This

would be at least somewhat analogous to the common practice with commercial fixed bed

catalytic reactors, in which an endothermic reaction is carried out in parallel in multiple narrow

tubes held between two tubesheets, with the heat source on the shell side.  Advantages of the

bayonet design include internal heat recuperation, the need for low-temperature connections

only, corrosion resistance, and low fabrication cost.  In fact, SiC bayonets are an off-the-shelf

item, since they are used commercially for thermowells[3].

## 3.    Analysis

### 3.1    *Heat requirement for the bayonet decomposition reactor*

As noted earlier, if the SDE operates at a cell potential of -0.6 V the balance of the HyS

cycle can consume no more than about 450 kJ/mol $H_2$ of high-temperature heat in order to be

---

[3] For example, Saint-Gobain Ceramics markets Hexoloy® sintered alpha silicon carbide thermowells that range
from 6 to 54 in (0.15 to 1.37 m) in length and from 0.375 to 1.5 in (0.0953 to 0.0381 m) in diameter.

competitive with water electrolysis.  Thus, it is important to establish what the heat requirement is for the bayonet reactor.

The heating requirement was determined by means of a pinch analysis.  The objective of this analysis was to quantify the high-temperature heating target, which provides a lower limit for the heat input needed to drive the decomposition reaction.  The Second Law of Thermodynamics guarantees that the actual heat consumption can only be greater than or equal to the target value.

Since this was a bounding calculation, there was no need to do a detailed heat transfer design.  Instead, the assumption was made that the bayonet design was adequate for achieving good heat transfer.  This means that the reaction can be accomplished with a practical bayonet length and that reasonable temperature differences can be attained.  For this calculation, a 25 °C (25 K) minimum difference between the temperature of the process fluid in the annulus and the temperature of the helium heat transfer medium flowing countercurrently across the bayonet surface was imposed.  A smaller, 10 °C (10 K) temperature approach between the annulus and center tube fluids was also used.

The pinch analysis assumed that the process fluid moves through the bayonet reactor in plug flow, and that the catalyst allows the decomposition reaction to proceed to thermodynamic equilibrium at the local pressure, temperature, and composition.  An Aspen Plus™ flowsheet model was devised to track the progress of a fluid element as it passes through the reactor, from the inlet, up the annulus and the catalyst bed, down the center tube, and to the outlet. Sufficiently small temperature increments were used (on the order of 10 °C or 10 K) to allow the construction of detailed heating and cooling curves (enthalpy as a function of temperature) for a determination of the heating target.

Aspen Technology, Inc. (AspenTech) provides its licensees an Oleum Data Package for use with Aspen Plus™ that provides accurate representation of $H_2SO_4$ properties and phase equilibria over the entire concentration range, from 0 through 100% $H_2SO_4$ to 100% sulfur trioxide ($SO_3$ or oleum). Unfortunately, the temperature range for this data package extends no higher than 150 °C (423 K), while the pressure is limited to about 2 bar. This limitation was removed by Mathias in work commissioned by General Atomics for modeling the SI cycle [17]. Mathias' work is in the public domain [18].

Mathias split his $H_2SO_4$ properties model into two temperature ranges. For temperatures below about 300 °C (573 K), he refit AspenTech's oleum model simultaneously to the vapor-liquid equilibrium correlation developed by Gmitro and Vermeulen [19] and to excess enthalpy [20] and heat capacity [21] data for $H_2SO_4$-$H_2O$ mixtures. Here the underlying Chen Electrolyte-NRTL (ELECNRTL) property method assumes that aqueous $H_2SO_4$ dissociates to form sulfate and bisulfate anions,

$$H_2SO_4(aq) + H_2O(l) \leftrightarrow H_3O^+ + HSO_4^- \tag{3}$$

$$HSO_4^- + H_2O(l) \leftrightarrow H_3O^+ + SO_4^{2-} \tag{4}$$
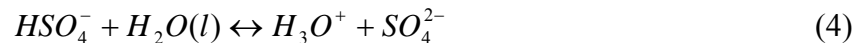
The model also includes a vapor phase dissociation equilibrium for $H_2SO_4$,

$$H_2SO_4(g) \rightarrow H_2O(g) + SO_3(g) \tag{5}$$
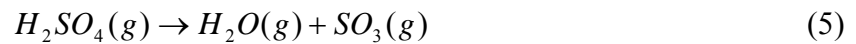
At higher temperatures (above 300 °C, or 573 K), the electrolyte model tends to break down, so Mathias replaced the aqueous dissociation equilibria of $H_2SO_4$ with a nonvolatile complex-forming equilibrium,

$$H_2SO_4(aq) + H_2O(l) \leftrightarrow 2IonPair \tag{6}$$

The postulated complex "IonPair" is assumed to be a molecular component with very low vapor pressure, so the model has no electrolytes. Equation (5) was left unchanged. Mathias fit this

model to the high-temperature, high-pressure data of Wüster [22] as well as to extrapolations of the lower temperature excess enthalpy and heat capacity data. Fig. 4, reproduced from Mathias' report [17], shows that the model matches Wüster's data very well.

For this work, Mathias' $H_2SO_4$ properties model was modified to take into account solubility data for $SO_2$ in aqueous $H_2SO_4$ that were not included in its original development. ($SO_2$ is treated as a HENRY_COMPS or supercritical component.) The modifications consisted of fitting interaction parameters for $SO_2$ with other aqueous species to the available data. Furthermore, the optimal transition from the low-temperature, electrolyte to high-temperature, complex-forming model was found to occur at 270 °C (543 K). (The smallest differences between enthalpies calculated using the two methods for a given temperature, pressure, and composition were typically observed around 270 °C, 543 K). Consequently, a switch from one properties model to the other is arbitrarily imposed whenever a stream temperature passes through 270 °C (543 K).

The Aspen Plus™ flowsheet used to set up the decomposition reactor pinch analysis is shown in Fig. 5. Concentrated sulfuric acid is fed at the upper left (stream 1). The blocks along the top row are intended to simulate sequentially the preheating, vaporization, superheating, and decomposition of sulfuric acid as it flows from the bottom of the annulus (left hand side) to the top (right hand side). The blocks along the bottom row simulate the cooling and partial condensing of the effluent from the annular catalyst bed as it flows from top (right hand side) to bottom (left hand side).

Simulation of sulfuric acid decomposition is complicated by the fact that the properties model includes both liquid (equations 3, 4, and 6) and vapor phase (equation 5) equilibrium reactions, and Aspen Plus™ Chemistry models can not account for vapor phase equilibria in the

apparent composition mode. Any reactions involving volatile species on the right hand side

must instead be placed in Reactions models, so only those blocks that can explicitly account for

chemical reactions (e.g. RCSTR, RGibbs, Radfrac) can correctly represent the high-temperature

decomposition of sulfuric acid. That is why the Aspen Plus™ flowsheet in Fig. 5 contains

RCSTR and RGibbs blocks instead of the Heater blocks one might reasonably expect to see.

Block HTR1 is a Heater block that uses the low-temperature properties model to

calculate the heat required to raise the temperature of the liquid feed (stream 1) to 270 °C (543

K), with the implicit assumption that the equation 5 reaction can be ignored. This is followed by

an RCSTR block (HTR2) using the high-temperature properties model to calculate the heat

required to vaporize stream 2 while allowing the vapor phase dissociation of $H_2SO_4$ to $H_2O$ and

$SO_3$ to proceed to equilibrium. A Design Spec is used to adjust the temperature of HTR2 such

that the liquid fraction of stream 3 is 2.5% (almost all-vapor). Block HTR3 is identical to HTR2

except that the specified temperature is 10 °C (K) higher, resulting in an all-vapor effluent

(stream 4). This arrangement establishes the boiling temperature range for the full pinch analysis

model. Block HTR4 is an RGibbs block that uses the high-temperature properties model to

calculate the heat required to raise the temperature of all-vapor stream 4 to the inlet temperature

of the annular catalyst bed, while allowing the vapor phase dissociation of $H_2SO_4$ to $H_2O$ and

$SO_3$ to continue toward equilibrium. The $SO_3$ decomposition reaction (equation 1b) takes place

in RGibbs block RXTR, and proceeds to equilibrium simultaneously with equation 5. (The

reactions of equations 1b and 5 are not explicitly stated in the RGibbs block specifications, but

are implicit in the composition of the individual blocks' Products and Inerts lists.)

Cooling of the decomposition product begins with RGibbs block CLR1, which has

specifications identical to those for block HTR4 except that the temperature is just above the dew

point of stream 7.  The dew point is determined using a Design Spec in conjunction with RCSTR

block CLR2 that adjusts the temperature of CLR2 such that the liquid fraction of stream 8 is

2.5% (almost all-vapor).  The other specifications for CLR2 are identical to those for HTR2 and

HTR3.  A Calculator block sets the temperature of CLR1 10 °C (K) higher than CLR2 in an

iterative calculation coupled with the Design Spec, guaranteeing an all-vapor condition for

stream 7.  This arrangement establishes the condensing temperature range for the full pinch

analysis model.  RCSTR block CLR3 is identical to CLR2 except that the specified temperature

is 270 °C (543 K), allowing transition from the high-temperature to the low-temperature

properties model.  Block CLR4 is a Heater block that uses the low-temperature properties model

to calculate the amount of cooling needed to lower the temperature of the vapor-liquid product

(stream 11) to the bayonet outlet temperature, with the implicit assumption that the equation 5

reaction is negligible.  A "dummy" RStoic reactor block (DMY) is used to recombine the trace

amounts of $SO_3$ in stream 10 with $H_2O$ to make $H_2SO_4$, returning the effluent composition to an

$H_2SO_4$ apparent basis.

The full bayonet reactor pinch analysis model contains many more blocks, which result

from a subdivision of blocks HTR1, HTR2, HTR4, RXTR, CLR1, CLR3, and CLR4 into

multiple, identical blocks in sequential order, with uniform block-to-block temperature

increments on the order of 10 °C (10 K), to allow the construction of detailed heating and

cooling curves.  For example, the liquid feed is heated to 270 °C (543 K) in a series of sixteen

heater blocks, each with an outlet temperature that is one-sixteenth of the difference between 270

°C (543 K) and the feed (stream 1) temperature higher than that of the preceding block.  Blocks

HTR2, HTR4, RXTR, CLR1, and CLR3 are likewise subdivided into 28, 12, 23, 41, and 23

identical blocks, respectively.  Block CLR4 is extended to 120 °C (393 K) and subdivided into

fifteen blocks to determine the cooling curve beyond the likely minimum outlet temperature, which is calculated from the pinch analysis.

Results (inlet and outlet temperatures and heat duty for each block) from the full bayonet reactor model were imported into Aspen HX-Net for the pinch analysis.  The heating target calculated from the resulting heating and cooling curves represents the minimum high-temperature heat input needed to carry out the decomposition reaction.  Fig. 6 illustrates a pinch analysis for the case of 80 wt% $H_2SO_4$ feed, with the bayonet operating at 86 bar pressure (negligible pressure drop between feed and product) and a peak internal (process) temperature of 870 °C (1143 K).  The catalyst bed inlet temperature is assumed to be 675 °C (948 K).  This combination of temperatures and pressure would be typical for an advanced, gas-cooled reactor heat source, operating at a 950 °C (1223 K) primary helium coolant outlet temperature and 87-bar outlet pressure, with a 50 °C (50 K) temperature drop across the intermediate heat exchanger [23].  High pressures are needed to minimize the pressure differential between the hot secondary helium coolant flowing outside the bayonet and the interior process stream.

The lower curve in Fig. 6 represents the temperature as a function of heat input (moving from left to right) for the fluid flowing through the annulus, while the upper curve tracks the temperature of the fluid flowing through the central tube of the bayonet as a function of heat removal (moving from right to left).  The pinch point represents the closest approach between the temperatures of the two fluids (10 °C or 10 K) flowing countercurrently under optimal heat transfer conditions.  The difference between the enthalpies of the two curves at the highest temperature (870 °C or 1143 K), is 328.6 kJ/mol $SO_2$.  This is the heating target, which is the lowest possible high-temperature heat requirement for a bayonet reactor operating at the stated conditions.  If all of the $SO_2$ is delivered to the SDE and consumed to produce $H_2$, this is

equivalent to 328.6 kJ/mol $H_2$.  Since this number is significantly less than 450 kJ/mol $H_2$, HyS

flowsheets using an SDE operating at a cell potential of -0.6 V coupled to a bayonet

decomposition reactor heated by an advanced nuclear heat source have the potential to

outperform water electrolysis.

Pinch analyses were performed for a variety of bayonet reactor operating conditions.  The

results are summarized in Figs. 7 and 8.  Fig. 7 plots the high-temperature heat target for $H_2SO_4$

decomposition over a wide range of feed concentrations (30 to 85%) for three different pressures

(57, 70, and 83 bar), while Fig. 8 plots the heat target over a more narrow range of feed

concentrations (70 to 85%) for four different pressures (56, 66, 76, and 86 bar).  In all cases, the

peak process temperature was 870 °C (1143 K), and the catalyst bed inlet temperature was 675

°C (948 K).  The lowest heating targets (on the order of 330 kJ/ mol $SO_2$) were obtained for feed

concentrations of 80% at all pressures.  Heating targets were below 450 kJ/ mol $SO_2$ provided

the feed concentration was $\geq$ 60 wt%.

Results of PEM SDE development experiments at SRNL suggest that 50 wt% is the

practical upper limit for anolyte acid concentration if a Nafion® or similar sulfonated

perfluoroploymer PEM is used.  That means the SDE product will need to be concentrated before

being fed to the bayonet reactor, or else the high-temperature heat requirement will be

impractical ($\geq$ 500 kJ/mol $SO_2$).  Consequently, a HyS process that uses PEM electrolysis in

conjunction with a bayonet decomposition reactor will need an acid concentration section,

preferably one that can make use of heat recovered from the other flowsheet sections to effect the

necessary separation.  It will also need a decomposition product handling system to separate and

remove $O_2$ co-product while feeding $SO_2$ and $H_2O$ to the SDE and recycling unconverted $H_2SO_4$

back to the bayonet.

### 3.2    *Integrating the bayonet reactor with a PEM SDE*

It is assumed that the SDE anolyte product is 50-wt% $H_2SO_4$ at 100 °C (373 K) and 20 bar, and that it contains unreacted $SO_2$ as well as traces of $O_2$. (Higher temperatures give better kinetics, but can't be tolerated by perfluoropolymer PEMs. Higher pressures favor $SO_2$ solubility, but are limited by $SO_2$ vapor pressure – two liquid phases could otherwise form in the SDE in some circumstances.) To integrate the SDE with a bayonet reactor, most of the anolyte will need to be recycled. The remaining product stream, containing one mole of $H_2SO_4$ for each mole of $H_2$ produced in the SDE, will be passed on. Unreacted $SO_2$ and trace $O_2$ will first need to be removed from this stream, along with about one-third (to yield 60 wt% $H_2SO_4$) to three-quarters (to yield 80 wt% $H_2SO_4$) of the water content. Similarly, the bayonet product will have to be cooled, unreacted $H_2SO_4$ recycled, $O_2$ removed, and the remaining $SO_2$ and water condensed and combined with recycled, spent anolyte to form fresh anolyte feed.

The simplest way to remove unreacted $SO_2$ and trace $O_2$ from the SDE product is to drop the pressure. This requires recompressing the predominantly $SO_2$ and trace $O_2$ vapor stream that is out-gassed so that it can be recycled to the SDE feed system. However, the shaft work required is not excessive, and the separation can be made without any heat input.

A variety of methods is available for concentrating the degassed SDE product. All require the expenditure of energy, some more than others. For example, 50% $H_2SO_4$ at 100 °C (373 K) and 20 bar can be concentrated to 75% $H_2SO_4$ by simply dropping the pressure to just under 0.05 bar while maintaining the temperature at 100 °C (373 K) requiring just over 169 kJ/mol $H_2SO_4$ heat input. Water boils off as a separate vapor phase. The pressure could also be maintained at 20 bar and the SDE product heated to 317 °C (590 K) instead to boil off the water.

This would take just over 246 kJ/mol $H_2SO_4$ heat input.  In either case, the heat required is excessive, and would cause the sum of the acid concentration and decomposition step heat duties to exceed the 450-kJ/mol $H_2$ practical upper limit before even considering the recycled undecomposed acid concentration step.  It is clear that a recuperative method is necessary.

Vacuum distillation with recuperative preheating/partial vaporization of the feed streams was chosen to concentrate the SDE product.  A two-stage steam ejector can be used to maintain column pressure, while temperatures can be kept high enough to allow use of cooling water in the condenser, yet low enough to allow metallic materials of construction.  Water removed in the concentration process can be condensed and recycled to the SDE feed system.  The vacuum column bottoms, containing concentrated sulfuric acid, can be easily pumped to the necessary pressure and fed directly to the bayonet reactor.

The bayonet reactor effluent can be readily separated into unreacted $H_2SO_4$ feed and the $SO_2/O_2$ product by doing a vapor/liquid split.  The acid can be recycled to the vacuum still, while the vapor can be further cooled and let down to the SDE pressure.  This will result in a three-phase system: wet liquid $SO_2$, a saturated solution of $SO_2$ in $H_2O$, and wet $O_2$ gas contaminated with $SO_2$.  The $O_2$ gas can be scrubbed with the water collected in the concentration process to remove most of the $SO_2$.   The two liquid phases can then be combined with that water and with recycled, spent anolyte to form fresh anolyte feed.

An important consideration is that since the SDE and bayonet reactor already pose significant technological challenges by themselves, the balance of the flowsheet should not introduce additional technical hurdles, but should only use proven technology.  This will help give performance projections much greater credibility.  The aforementioned flowsheet choices accomplish this goal.

# 4.    Results and discussion

## *4.1    The PEM SDE / Bayonet Reactor Hybrid Sulfur flowsheet*

An Aspen Plus™ flowsheet was prepared that incorporates the elements described in the preceding section.  This flowsheet is illustrated in Fig. 9.  Stream compositions and conditions are detailed in Table 2.  The basis is a 1-kmol/sec $H_2$ production rate.

While a modification of Mathias' $H_2SO_4$ properties model worked very well for bayonet decomposition reactor simulations, it was not set up to handle some parts of the HyS flowsheet, particularly those where $SO_2$ is present as a separate, nonaqueous liquid phase and can no longer be treated as a supercritical component.  Furthermore, the need to transition between the low- and high-temperature models for streams that are heated or cooled through 270 °C (543 K) can cause enthalpy mismatches.  For these reasons, the flowsheet simulations were done instead using OLI Systems, Inc.'s Mixed Solvent Electrolyte (MSE) model, which has been shown to represent the $H_2SO_4$-$H_2O$ system very well over its entire composition range and at temperatures as high as 500 °C (773 K) [24].  (The Aspen-OLI interface allows use of the OLI Engine from within Aspen Plus™.)  Spot checks of the OLI MSE model's representations of $SO_2$-$H_2O$ and $SO_2$-$H_2SO_4$-$H_2O$ vapor-liquid and liquid-liquid equilibria against the available data showed generally good agreement (e.g. see Figs. 10 [25,26,27] and 11 [28),29,30]).

Returning to the flowsheet, the SDE, block EL-01, is on the left-hand side.  Stream 1 is the $H_2O$ feed to the cathode side, while stream 2 is 15.5 wt% $SO_2$ dissolved in 43.5 wt% $H_2SO_4$, fed to the anode side. Both streams are assumed to be at 21 bar pressure, and the SDE is assumed to impart a pressure drop of 1 bar due to frictional losses.  The composition of stream 2 was set such that the quantity of dissolved $SO_2$ is just below the saturation point (beyond which a

separate liquid $SO_2$ phase would form) and that the concentration of $H_2SO_4$ in the anolyte

product following the reaction would be 50% by weight (not including $SO_2$).

Since a detailed model of the SDE has not yet been developed, it was treated as a "black

box" in which the following changes take place:

- A net flux of $H_2O$ from the cathode to the anode (assumed to be 1 kmol $H_2O$ / kmol $SO_2$

  reacted) is imposed.  This results from the difference in water activity across the PEM.

- Reaction occurs between $SO_2$ and $H_2O$ to make $H_2SO_4$ and $H_2$ via equation (2) with an

  assumed $SO_2$ conversion of 40% (i.e. the anolyte feed contains 150% excess $SO_2$).

- All of the $H_2$ product exits the cathode with the remaining water via stream 3.

- All remaining constituents exit the anode via stream 11.

- To simulate no heat lost to the surroundings, the temperatures of streams 3 and 11 are

  assumed to be identical and are calculated such that the enthalpy change between the feed

  (1 and 2) and product (3 and 11) streams is equal to the electrical work performed with a

  cell potential of 0.6 V.  (This allows the heat dissipated due to the overpotential to be

  removed downstream.)

- Streams 3 and 11 are assumed to exit the SDE at a pressure of 20 bar.

The temperature of the SDE (and streams 3 and 11) is maintained at 100 °C (373 K) by adjusting

the temperature of anolyte feed stream 2 using heat exchanger HX-06.  Experimental evidence

for the diffusion of water from the cathode to the anode in a PEM SDE has been provided by

Weidner and co-workers [31] at the University of South Carolina (USC).  The assumed flux of 1

kmol $H_2O$ / kmol $SO_2$ reacted is an estimate that needs to be refined with further experiments.

The assumed $SO_2$ conversion of 40% is a design goal based on experimental results at

SRNL and USC.  Higher conversion means less material to be recycled, but at the expense of

higher cell potential due to lower average $SO_2$ concentration at the anode. Conversions in excess of 20% have been routinely achieved in SDE development experiments at SRNL, and over 50% at USC using gaseous $SO_2$ feed. The optimum value of conversion will be determined by a trade-off between cell potential and recycle effects once the relationship between conversion and cell potential is established.

A mixture of $H_2$ and $H_2O$ exits the cathode side (stream 3) at 100 °C (373 K) and 20 bar and is cooled by interchange with stream 17 to 77 °C (350 K) in heat exchanger HX-01, maintaining a 10 °C (10 K) minimum temperature difference. The vapor phase (stream 5) is removed in knock-out drum KO-01 and fed to the $H_2$ Dryer (DR-01), which is cooled to 40 °C (313 K) with cooling water and is assumed to remove all of the $H_2O$ (stream 8). Pure, dry $H_2$ is produced (stream 6) at 40 °C (313 K) and 20 bar. The "feedstock" $H_2O$ that is to be split into $H_2$ and $O_2$ (stream 9) is combined with recycled $H_2O$ (stream 7) and that removed by the dryer (stream 8) and pumped back to the cathode feed by means of the cathode feed pump (PP-01). Since the flux of water across the PEM from the cathode to the anode due to diffusion is assumed to be exactly 1 kmol $H_2O$ / kmol $SO_2$, this closes the water-splitting material balance.

A detailed design for the $H_2$ Dryer was not made, and regeneration requirements were not taken into account. Simple cooling from 77 °C to 40 °C (350 K to 313 K) should remove most of the water by condensation; the remainder could be absorbed by a molecular sieve. This simplification is not expected to have a significant impact on cost or energy efficiency.

The anolyte product (stream 11), containing 9.1 wt% unreacted $SO_2$ dissolved in 50.1 wt% $H_2SO_4$, is split at SP-01, sending enough $H_2SO_4$ to decomposition via stream 12 to make all of the $SO_2$ needed for the SDE. The remainder (representing 80% of the anolyte effluent) is recycled to the anolyte prep tank (TK-01) via stream 48, which is first cooled to 80 °C (353 K)

by interchange with stream 17 in heat exchanger HX-05, maintaining a 10 °C (10 K) minimum temperature difference.

The pressure of the anolyte product is dropped in three stages before being fed to the Vacuum Column (TO-01).  Adiabatic throttling valve VV-01 drops the pressure to atmospheric, allowing over 90% of the $SO_2$ and all but a trace of the dissolved $O_2$ to be removed in knock-out drum KO-02 via stream 52, along with some $H_2O$.  Next, the pressure is dropped to slightly over 0.3 bar via adiabatic throttling valve VV-02.  A steam-driven vacuum ejector (EJ-01) provides the suction needed to maintain vacuum.  Nearly 90% of the remaining $SO_2$ and a little more $H_2O$ are removed in knock-out drum KO-03 via stream 69.  Finally, the pressure is dropped to match the feed stage pressure in the Vacuum Column (0.11 bar) by means of adiabatic throttling valve VV-03.  The resulting 50.7% $H_2SO_4$ stream (number 17) is heated and partially vaporized by interchange with six other streams in heat exchanger HX-02, maintaining a 10 °C (10 K) minimum temperature difference with all of them.  When fed to the Vacuum Column on equilibrium stage 5, stream 18 is at 94.4 °C (367.6 K) and has a vapor fraction of almost 37%.

The Vacuum Column is maintained at an overhead pressure of 0.09 bar by means of the second-stage steam ejector, EJ-02.  The pressure drop from bottom to top is assumed to be 0.04 bar, so the bottoms is at 0.13 bar[4].  TO-01 has 9 equilibrium stages, including a partial condenser (stage 1) and a kettle reboiler (stage 9).  The reflux ratio (reflux/distillate) is 0.1, and the distillate vapor fraction is 0.001.  A bottoms concentration of 75% $H_2SO_4$ is achieved by adjusting the distillate rate (to just under 4.4 kmol/sec).  Under these conditions, the bottoms is at 122.9 °C (396 K) and requires 75.5 kJ/mol $H_2$ heating, which can be supplied with a low-pressure steam

---

[4] Vendor-prepared rating calculations indicate that a column pressure drop as low as 0.02 bar should be possible if FLEXERAMIC® 88 ceramic or FLEXIPAC® HC 2Y metallic structured packing from Koch-Glitsch is used.

utility.  The overhead is at 40 °C (313 K) and requires 210.5 kJ/mol $H_2$ cooling, all of which could be provided using a conventional cooling water system[5].

Bottoms product from the Vacuum Column (stream 19) is 75 wt% $H_2SO_4$ at 122.9 °C (396 K) and 0.13 bar.  It is pumped directly to the Bayonet Reactor (RX-01) by means of pump PP-02, which raises the pressure to 86 bar.  A separate simulation (detailed in Section 5 above) was used to establish the minimum high-temperature heating target for RX-01, resulting in the requirement of 340.3 kJ/mol $H_2$, which would need to be provided by the high-temperature nuclear heat source.  The fractional conversion of $H_2SO_4$ was 48.1%, and the effluent temperature was 254.7 °C (528 K) with a vapor fraction of about 20.4%.

The product of the Bayonet Reactor (stream 21) is separated into its liquid (stream 22) and vapor phase (stream 31) components in knock-out drum KO-04.  The pressure of the liquid product is then dropped to 21 bar by means of adiabatic throttling valve VV-04, allowing about 80% of the dissolved $SO_2$ and 99% of the dissolved $O_2$ to be removed in knock-out drum KO-05. The remaining liquid (stream 24) is a 59.3 wt% $H_2SO_4$ solution at 233.4 °C (507 K) that can be recycled to the Vacuum Column.  The vapor that was removed (stream 47) contains some of the $SO_2$ and $O_2$ products of the decomposition reaction.  It is sent to the $SO_2$ Absorber (TO-02) for separation.

The recycled, unconverted $H_2SO_4$ stream (number 24) is dropped in pressure before being fed to the Vacuum Column in three stages in a manner identical to the SDE anolyte product.  Adiabatic throttling valve VV-05 decreases the pressure to atmospheric, allowing over 99% of the $SO_2$ and all but a trace of the dissolved $O_2$ to be removed in knock-out drum KO-06 via stream 54, along with about 22% of the $H_2O$.  Next, the pressure is dropped to slightly over

---

[5] This may be impossible to achieve in some climates during the summer, since it implies the cooling water supply temperature does not exceed 30 °C (303 K).

0.3 bar via adiabatic throttling valve VV-06.  Nearly 99% of the remaining $SO_2$ and more $H_2O$ are removed in knock-out drum KO-07 via stream 71.  Finally, the pressure is dropped to match the feed stage pressure in the Vacuum Column (0.13 bar) by means of adiabatic throttling valve VV-07.  The now 67.1 wt% $H_2SO_4$ stream (number 29) is heated and partially vaporized by interchange with two other streams in heat exchanger HX-03, maintaining a 10 °C (10 K) minimum temperature difference with both.  When fed to the Vacuum Column on equilibrium stage 8, stream 30 is at 114.6 °C (387.8 K) and has a vapor fraction of 13.5%.

Hot (254.7 °C, 5278 K) vapor from the Bayonet Reactor (stream 31) is cooled to 40 °C (313 K) and partially condensed in three steps (by heat exchangers HX-04A, HX-04B, and HX-04C), after which it is separated into one vapor and two liquid phases in knock-out KO-08.  The lighter liquid phase consists of $H_2O$ with 27.3 wt% dissolved $SO_2$ and a small amount of $O_2$.  The heavier phase is liquid $SO_2$ containing 3.7 wt% $H_2O$ and a small amount of $O_2$.  HX-04A is cooled by interchange with the recycled acid feed to the Vacuum Column (HX-03), while HX-04B interchanges with the anolyte product feed to the Vacuum Column (HX-02).  HX-04C rejects heat to cooling water.  In practice, it would not be necessary to separate the two liquid phases in KO-08, since both are ultimately sent to the Anolyte Prep Tank.  However, the split is shown to make the point that separate aqueous and $SO_2$ phases can and do exist at these conditions.

The vapor and liquid effluents from KO-08 are let down in pressure from 86 bar to 21 bar via adiabatic throttling valves VV-08, VV-09, and VV-10, which leads to further phase changes.  The vapor phases are separated from the residual liquids in knock-outs KO-09, KO-10, and KO-11, and fed to the bottom of the $SO_2$ Absorber, while the liquid phases are sent to the Anolyte Prep Tank.

Returning to the acid concentration part of the flowsheet, the second-stage ejector (EJ-02) effluent (stream 85) is cooled to 40 °C (313 K) with cooling water in heat exchanger HX-12 and the condensate (stream 86) pumped to waste by means of pump PP-09. This helps ensure that any contaminants that may have entered with the steam (stream 84) are purged from the system. The remaining vapors (stream 89) are sent to knock-out KO-14, which is maintained near 0.3 bar by means of the first-stage ejector, EJ-01. KO-14 also receives the partially condensed vapors from knock-outs KO-03 (stream 70) and KO-07 (stream 73), after having first been cooled with cooling water to 40 °C (313 K) by heat exchangers HX-09 and HX-10B . Some of the heat released by condensation (in heat exchanger HX-10A) is transferred by interchange to HX-02. The aqueous phase removed by KO-14 (stream 74) is pumped to the $SO_2$ Absorber by means of pump PP-07, where it is fed on stage 3.

First-stage ejector (EJ-01) effluent (stream 78) is cooled to 40 °C (313 K) with cooling water in heat exchanger HX-11 and the condensate (stream 79) sent to waste. The remaining vapors (stream 80) are sent to an atmospheric pressure knock-out, KO-12. This knock-out also receives partially condensed vapors from knock-outs KO-02 and KO-06. Vapors removed in knock-out KO-02 (stream 52) are first cooled to 40 °C (313 K) with cooling water by heat exchanger HX-07, while those removed in knock-out KO-06 (stream 54) are cooled to 40 °C (313 K) in a series of three heat exchangers: HX-08A, which drops the temperature to 110.5 °C (384 K) by interchange with HX-03; HX-008B, which further cools to 77 °C (350 K) by interchange with HX-02; and HX-08C, which uses cooling water to achieve an outlet temperature of 40 °C (313 K).

The liquid recovered in knock-out KO-12 (stream 67) is a dilute solution of $SO_2$ in $H_2O$ (4.8% by weight). It is pumped to the $SO_2$ Absorber by means of pump PP-06, where it is fed on

stage 5.  The vapor removed by the knock-out (stream 58) is a moist $SO_2$ stream (7.3 mol% $H_2O$) containing about 0.3 mol% $O_2$.  It needs to be compressed to 21 bar before it can be fed to the bottom of the $SO_2$ Absorber.  This is accomplished with the three-stage $SO_2$ Recycle Compressor, CO-01, which has intercoolers and knock-outs that cool the outlet of each stage to 40 °C (313 K) and remove any condensate.

The first stage raises the pressure to 2.78 bar.  About 5% (by volume) of the feed condenses and is removed as a 12.9% (by weight) solution of $SO_2$ in $H_2O$ (stream 62) in the first stage intercooler and knock-out.  Pump PP-04 is used to send this stream to the Anolyte Prep Tank.  The second stage raises the pressure to 7.65 bar.  Most of the effluent from this stage condenses in the intercooler and is removed by the knock-out (stream 64) as nearly pure liquid $SO_2$ containing 0.8% $H_2O$ by weight and a trace of $O_2$.  Pump PP-05 sends this stream to the Anolyte Prep Tank.  Partially condensed effluent from the last stage (stream 59) is fed to knock-out KO-13. Of the original feed to CO-01 (stream 58), less than 1% (by volume) remains in the vapor phase (stream 66) and is fed to the bottom of the $SO_2$ Absorber; a little more than twice that amount is removed as condensate (stream 60) and sent to the Anolyte Prep Tank.  Stream 66 is roughly 65% $O_2$/35% $SO_2$ (by volume), while stream 60 is 99.9% $SO_2$ (by weight), with minor amounts of $O_2$ and $H_2O$.

The $SO_2$ Absorber is an eight-equilibrium stage vapor-liquid fractionation device.  It operates at 21 bar pressure with an assumed negligible pressure drop.  Liquid distillate from the Vacuum Column (stream 81) is fed by means of pump PP-08 to the top stage.  This stream is 99.9% $H_2O$ by weight, with 0.1% $SO_2$ at 40°C (313 K).  Effluent from the second-stage ejector knock-out (stream 75), containing 98.7% $H_2O$ by weight, with 1.3% $SO_2$ at 41 °C (314 K) is fed to stage 3.  The first-stage ejector knock-out effluent (stream 68) is routed to stage 5. It contains

95.2% $H_2O$ by weight, with 4.8% $SO_2$ at 40 °C (313 K).  Vapor effluents from five knock-outs and the Anolyte Prep Tank vent are fed to the bottom.  $SO_2$ is scrubbed from the vapor phase as it rises up the Absorber, encountering water with progressively less dissolved $SO_2$.  The overhead product (stream 90) is 98.7% $O_2$ (by volume) at 41 °C (314 K) and 21 bar, with 0.5% $H_2O$ and 0.8% $SO_2$.  It is fed to the $O_2$ Dryer (DR-02), where the $H_2O$ and $SO_2$ are removed (stream 93) and routed to the Anolyte Prep Tank, leaving a pure $O_2$ product (stream 91) at 40 °C (313 K) and 21 bar.  The $SO_2$ Absorber bottoms stream (92) contains 14.1% (by weight) $SO_2$ in $H_2O$ at 82 °C (355 K) and 21 bar, with traces of $O_2$ and $H_2SO_4$.  It is sent to the Anolyte Prep Tank.

As was true for the $H_2$ Dryer, a detailed design for the $O_2$ Dryer was not made, and regeneration requirements were not taken into account.  Selective absorption of $SO_2$ and $H_2O$ by a molecular sieve would be the likely mechanism.  This simplification is likewise not expected to significantly impact capital cost or energy efficiency.

All of the $SO_2$ produced by the decomposition of $H_2SO_4$, as well as that recovered from the SDE anolyte effluent and any liquids end up in the Anolyte Prep Tank.  The resulting liquid (stream 51) is a 43.5% $H_2SO_4$ solution (by weight), containing 15.5% $SO_2$ at a temperature of 84.7 °C (358 K) and a pressure of 21 bar.  This is fed to the SDE anode after adjusting the temperature in heat exchanger HX-06 (by interchange with stream 17 via HX-02) to achieve a 100 °C (373 K) SDE outlet temperature.  The anolyte feed (stream 2) temperature is 78.8 °C (352 K).

Make-up sulfuric acid is added to the Anolyte Prep Tank as needed to compensate for $SO_2$ and $H_2O$ losses due to the ejector blow-downs. (More water is wasted via stream 88, which also contains some $SO_2$, than enters with streams 77 and 84.)  The quantity of make-up needed is

very small (about 0.008 kmol total/kmol $H_2$ product) and the sulfur content, at 23.6% $H_2SO_4$ (by weight), corresponds to only about 0.0004 kmol S/kmol $H_2$ product.

## *4.2    Flowsheet energy requirements*

Heat exchanger specifications are presented in Table 3.  Looking at all the entries, heat input is required in only two places: the Bayonet Reactor (RX-01) and the Vacuum Column (TO-01) reboiler.  The Bayonet Reactor obviously needs a high-temperature heat source, with heat input of 340.3 kJ/mol $H_2$.  The reboiler, on the other hand, could use low-temperature heat, since it operates in the 100 to 125 °C (373 to 398 K) range.  The amount needed is only 75.5 kJ/mol $H_2$.  A grand total of 252.9 kJ/mol $H_2$ waste heat is rejected to cooling water, over 80% of which occurs in the Vacuum Column condenser.  Recuperation is responsible for 130.5 kJ/mol $H_2$ worth of heating in HX-02 and 31.8 kJ/mol $H_2$ in HX-03.

A small quantity of steam is also needed to drive the vacuum ejectors (streams 77 and 84, estimated using a one-to-one molar entrainment ratio).  The combined amount was calculated at about 0.0277 kmol/sec, which corresponds to a 1.31-kJ/mol $H_2$ heat duty (from the enthalpy difference between boiler feed water at 40°C, or 313 K, and 7.91-bar steam).  This is two orders of magnitude smaller than the Bayonet Reactor duty, so it has little impact on the efficiency calculation.  A more rigorous ejector design should be undertaken to confirm the validity of this simplification.

Electric power requirements are detailed in Table 4.  A total of 120.9 kJ/mol $H_2$ electric energy is used in the flowsheet, nearly all of it (115.8 kJ/mol $H_2$) by the SDE.  The $SO_2$ Recycle Compressor is responsible for most of the rest, about 2.8 kJ/mol $H_2$.  It should be kept in mind that frictional losses due to flow through piping and equipment have been largely ignored, so the

actual pumping requirement will be somewhat higher.  If a thermal-to-electric conversion efficiency of 45% is assumed, the total electric power requirement corresponds to a heat input of 268.7 kJ/mol $H_2$.

Adding together the high- and low-temperature heat requirements, the total heat supplied to the process is 417.1 kJ/mol $H_2$.  This meets the ≤450 kJ/mol $H_2$ goal discussed in Section 2.2.  When the thermal equivalent of the power requirement is added, this flowsheet consumes a total of 685.8 kJ/mol $H_2$, which compares favorably with HTGR-powered water electrolysis at 791 kJ/mol $H_2$.  The comparison is made more favorable if it is acknowledged that a significant portion of the heat can be supplied by another source.  The 76.8 kJ/mol $H_2$ heat duty needed by the Vacuum Column reboiler and the steam ejectors could be supplied by a low-pressure steam utility with a non-HTGR primary source.  In that case, the quantity of HTGR heat needed by this flowsheet would be only 609 kJ/mol $H_2$ (including the thermal energy needed for electricity production).

## *4.3    Discussion*

The flowsheet presented above combines a PEM SDE with a bayonet reactor, using only proven chemical process technology.  If the SDE and the high-temperature decomposition reactor perform as projected (-0.6 V cell potential, 40% conversion, 50 wt% $H_2SO_4$ product; 25 °C or K minimum temperature difference between He coolant and process stream, 10 °C or K minimum temperature difference between process streams, adequate heat transfer characteristics) the flowsheet process will produce $H_2$ and $O_2$ from $H_2O$ while consuming 340.3 kJ/mol $H_2$ high-temperature heat, 75.5 kJ/mol $H_2$ low-temperature heat, 1.31 kJ/mol $H_2$ low-pressure steam, and 120.9 kJ/mol $H_2$ electric power.  Should the ultimate source of all of this energy be an HTGR

(process heat as well as electricity at 45% conversion efficiency), the net thermal efficiency would be 35.3% (LHV basis, or 41.7%, HHV basis). This is significantly more efficient than alkaline electrolysis (4.8 kWh/Nm$^3$ H$_2$) or PEM electrolysis (4.4 kWh/Nm$^3$ H$_2$) coupled with HTGR power (28.1% or 30.7%, LHV basis, respectively).

In reality, the efficiency difference may be even larger than it seems. HTGR electric power (at least initially) will likely be more expensive than conventional BWR/PWR power. Passive safety constraints limit individual HTGR reactors to no more than about 600 MW$_{th}$ in size, while the lower-temperature BWR/PWR reactors can be significantly larger [32][6]. Economies of scale help to make the otherwise less efficient BWR/PWR power less expensive. Eventually, standardized design, factory production, and higher efficiency may overcome this limitation, but not until a number of HTGR plants have been built. Consequently, water electrolysis is initially more likely to be powered by electricity made using water-cooled reactors, which can not achieve the temperatures needed for the H$_2$SO$_4$ decomposition step in sulfur cycles. This means the net thermal efficiency (including electric power generation) for H$_2$ production by water electrolysis will actually be approximately 22.4%.

It also means that HTGRs will initially likely be used primarily for process heat, and that the HyS SDE will probably be powered by electricity from the grid. In that case, the net thermal efficiency for the HyS flowsheet process will be 30.9% (LHV basis), assuming grid power is produced by water-cooled reactors. This compares very favorably with the 22.4% efficiency calculated for water electrolysis.

In any event, it is the unit cost of H$_2$ production ($/kg H$_2$) that will ultimately determine whether the HyS process will be commercialized. If water can be split into H$_2$ and O$_2$ more

---

[6] The European Pressurized Water Reactor (EPR) under construction in Finland is rated at 4,300 MW$_{th}$ and 1,600 MW$_e$ [32].

economically by this method than by simple electrolysis or other competing process, then HyS

plants will be the preferred choice for $H_2$ production using nuclear power. A detailed estimate of

the unit cost of $H_2$ production using the HyS process will be the subject of a future paper.

One additional caveat needs to be kept in mind when considering these results. Moving

hot, pressurized helium through ductwork and heat exchangers requires a significant expenditure

of energy. As noted in a DOE Nuclear Energy Research Initiative (NERI) study published in

2006 [33], the primary and secondary loop circulators for a 600-$MW_{th}$ HTGR coupled with a

Sulfur-Iodine cycle process would require on the order of 25 $MW_e$ electric power. Comparable

power requirements would be expected for a HyS process. While the work performed on the

helium heat transfer fluid is eventually recovered in the form of heat, the conversion loss that

occurs with electric power generation imposes an additional energy penalty that should be

included in the efficiency calculation. However, the actual power requirement depends on the

design of the nuclear heat source, which was not part of this work. The detailed $H_2$ production

cost estimate being prepared for a future paper will include the HTGR as well as the helium heat

transfer loops.

Finally, 252.9 kJ/mol $H_2$ waste heat is rejected to cooling water. This too will require

some expenditure of electric energy (to pump water to and from the cooling tower), but the

amount should be much smaller than that needed for the reactor heat transfer loops. The cooling

water system will also be included in the future paper.

## *4.4*    *Assumptions*

The flowsheet presented above relies on a series of assumptions for its predicted performance. While these have been clearly stated, a brief discussion as to their implications is in order.

Perhaps the most critical assumption is that the properties models used for flowsheet calculations accurately represent the $H_2SO_4$ - $H_2O$ - $SO_3$ - $SO_2$ - $O_2$ system. This premise is valid for the OLI MSE $H_2SO_4$ - $H_2O$ - $SO_3$ model [24]. Mathias' high-temperature extension of AspenTech's Oleum Data Package [17] also provides a sufficiently good representation of $H_2SO_4$ - $H_2O$ - $SO_3$ properties. Accurate models for the solubility/miscibility of $SO_2$ in/with mixtures of $H_2SO_4$ and $H_2O$, however, are still lacking. Figs. 10 and 11 show that while the OLI MSE model gives generally good agreement with the available data for this ternary, the fit could be much better. As for $O_2$, little attention has been paid to its solubility in $H_2SO_4$ or $SO_2$. These shortcomings, while not serious enough to have a material effect on the outcome of this work, will need to be addressed in future HyS process development efforts.

Another crucial assumption is that heat transfer can be achieved as needed in the high-temperature decomposition reactor in order to achieve the specified approach temperatures. Removing heat transfer from consideration allows a pinch analysis to establish the reactor performance limit dictated by thermodynamics, i.e. determine the high-temperature heating target. This is useful in determining the bounds for reactor operating conditions and performance. Results demonstrate that the bayonet concept has the potential to decompose sulfuric acid efficiently enough for a practical HyS process. Furthermore, the selected approach temperatures are consistent with good engineering practice. A coupled heat transfer analysis still needs to be performed, however, to verify that the concept can be made to work using a hot

helium heat transfer medium and with practical reactor dimensions, and to provide a design basis for a capital cost estimate.

Flowsheet calculations also assume that the high-temperature decomposition reaction proceeds to thermodynamic equilibrium.  If conversion were to fall short of equilibrium, the recycle rate of unconverted acid would increase, raising the Vacuum Column reboiler duty by a small amount.  The decomposition process is catalytic, so it is not unreasonable to expect that a sufficient volume of catalyst could allow the reaction to approach equilibrium.  Consequently, this is not an unreasonable assumption for a bounding calculation.  The reader should be aware that the actual conversion in the bayonet reactor could be somewhat less than that shown.

Absent a phenomenological model of the electrolyzer, SDE operation has been characterized using development performance targets, i.e. the SDE is assumed to operate at a fixed cell potential of -0.6 V, with a fixed $SO_2$ conversion of 40%, and at a fixed 50-wt% $H_2SO_4$ product composition.  If these targets can not be met, the efficiency advantage of HyS over water electrolysis will be diminished.  The conversion target should be the easiest to achieve, while the cell potential will likely be the hardest.  An SDE unit operation model that can be incorporated into the flowsheet and that relates these cell performance measures to input parameters would help determine how much these targets can be relaxed.  Such a model will need to be built for future development efforts.

The heat duties calculated for blocks HX-02 and HX-03 represent target values as determined by pinch analysis.  A practical heat exchanger network will need to be designed for the heat recovery scheme used by these blocks before a capital cost can be estimated for the flowsheet.

The flowsheet ignores piping and vessel pressure drops.  These will add to the actual power requirement (due to the need for pumping), but the increase should be small enough to disregard for now.  Furthermore, a uniform 10 °C (10 K) minimum temperature difference for process heat exchange is assumed throughout.  Optimal minimum temperature differences will vary from exchanger to exchanger, but this is a reasonable starting point for the conceptual design of a process in which energy recovery is at a premium.  One significant exception was the assumption of a 25 °C/K minimum temperature difference between the process fluid in the bayonet reactor and the helium heating stream.

Finally, the assumption that process streams can be cooled to 40 °C (313 K) with cooling water implies that cooling water is available year-round at 30 °C (303 K) or lower temperature.  This may be somewhat geographically limiting, but it allows the Vacuum Column to be operated without a refrigerated condenser.  The effect of increasing the summer cooling water temperature above 30 °C (303 K) will need to be evaluated for operation in hot climates.

# 5.     Summary and Conclusions

The HyS cycle splits $H_2O$ into $H_2$ and $O_2$ by combining the high-temperature, endothermic, catalytic decomposition of $H_2SO_4$ into $H_2O$, $SO_2$, and $O_2$ with $SO_2$-depolarized electrolysis that regenerates $H_2SO_4$.  A HyS process flowsheet has been developed for use with electric power and high-temperature heat sources that combines the PEM SDE technology being developed at SRNL with bayonet reactor $H_2SO_4$ decomposition technology being developed at SNL.  Conventional water electrolysis was proposed as a benchmark against which to compare this HyS cycle.  If electricity is available at a 45% heat-to-power conversion efficiency (e.g. HTGR with Brayton cycle PCU), water electrolysis could be used to make $H_2$ for a net energy

consumption of perhaps as little as 791 kJ/mol $H_2$.  Development goals for SRNL's PEM SDE include sustained operation at a cell potential of -0.6 V, which was shown to be equivalent to a 258-kJ/mol $H_2$ primary energy source.  This leaves a margin of 791 kJ –258 kJ = 533 kJ heat per mol $H_2$ product for the $H_2SO_4$ decomposition step in order to match the water electrolysis efficiency.  A goal of ≤450 kJ/mol $H_2$ was established to provide an edge.

A pinch analysis was used to establish high-temperature heating targets for the decomposition reactor as a function of pressure and $H_2SO_4$ feed concentration.  Results of the analysis showed that heating targets were below 450 kJ/ mol $SO_2$ for feed concentration ≥ 60 wt% and that increasing pressure decreases the target.  This requires that the SDE product with its maximum concentration of 50 wt% be concentrated before being fed to the bayonet reactor to meet the high-temperature heat requirement goal.

Vacuum distillation with recuperative preheating/partial vaporization of the feed streams and using a two-stage steam ejector was chosen to concentrate the SDE product.  Temperatures could be kept high enough to allow use of cooling water in the condenser, yet low enough to allow metallic materials of construction.  Only proven process technology was utilized, leaving the SDE and the bayonet reactor as the only major components that need development.

The resulting flowsheet, illustrated in Fig. 9, and with stream and equipment performance data tabulated in Tables 2 through 4, requires 340.3 kJ/mol $H_2$ high-temperature heat, 75.5 kJ/mol $H_2$ low-temperature heat, 1.31 kJ/mol $H_2$ low-pressure steam, and 120.9 kJ/mol $H_2$ electric power.  (If a 45% heat-to-power conversion efficiency is assumed, the electric power corresponds to a primary energy input of 268.7 kJ/mol $H_2$.)  Adding together the heat requirements and the thermal equivalent of the power requirement, it consumes a total of 685.8 kJ/mol $H_2$, which compares favorably with HTGR-powered electrolysis at 791 kJ/mol $H_2$.  When

conventional nuclear reactors are assumed to be the source of electric power, the HyS process has an even larger advantage over water electrolysis (783 kJ/mol $H_2$ versus 1,080 kJ/mol $H_2$, respectively).

Based on this result, the HyS cycle should be competitive with water electrolysis as a means of producing $H_2$ by water-splitting on a massive scale. It is a necessary prerequisite for commercializing the HyS cycle, that its projected $H_2$ production cost be lower than that attainable with competing technologies, especially conventional water electrolysis. For a more definitive determination, a detailed economic analysis will be needed, including the cost of building and operating the coupled nuclear heat source. This will be the subject of a future study, which will quantify the cost of $H_2$ production (\$/kg $H_2$). It is hoped that the detailed process flowsheet design and efficiency estimates presented here will contribute to a better understanding of the current status and future promise of the HyS cycle as a potential major component of a Hydrogen Economy.

# Acknowledgements

# References

1.  The Hydrogen Economy; Opportunities, Costs, Barriers, and R&D Needs. Washington, DC: National Academy of Engineering, 2004.

2.  U.S. Department of Energy, Energy Information Administration. Annual Energy Outlook 2008. Report No. DOE/EIA-0383(2008). http://www.eia.doe.gov/oiaf/aeo/, May 27, 2008.

3.  Brecher LE, Wu CK. Electrolytic decomposition of water. Westinghouse Electric Corp., US Patent No. 3888750, 1975.

4.  Farbman GH. The conceptual design of an integrated nuclear-hydrogen production plant using the sulfur cycle water decomposition system. NASA Contractor Report, NASA-CR-134976, 1976.

5.  Lu PWT, Ammon RL, Parker GH. A study on the electrolysis of sulfur dioxide and water for the sulfur cycle hydrogen production process. NASA Contractor Report, NASA-CR-163517, 1980.

6.  Parker GH. Solar thermal hydrogen production process. Final Report from Westinghouse Electric Corp. to US DOE, DOE/ET/20608-1, 1983.

7.  Brecher LE, Spewock S, Warde CJ. The Westinghouse Sulfur Cycle for the thermochemical decomposition of water. Int J Hydrogen Energy 1977;2(1):7-15.

8.  Bard AJ, Parsons R, Jordan J. Standard Potentials in Aqueous Solutions. New York: Marcel-Dekker, 1985.

9.  Bratsch SG. Standard Electrode Potentials and Temperature Coefficients in Water at 298.15K. J Phys Chem Ref Data 1989;18:1-21.

10. Lu PWT, Garcia ER, Ammon RL. Recent developments in the technology of sulphur dioxide depolarized electrolysis. J Appl Electrochem 1981;11:347-355.

11. Norsk Hydro Electrolysers AS. High Pressure Electrolysers: 10–60 Nm$^3$/h. http://www4.hydro.com/electrolysers/en/products/range/high_pressure_electrolyser/, February 25, 2008.

12. Norsk Hydro Electrolysers AS. Product development–the shape of things to come. http://www4.hydro.com/electrolysers/en/products/product_development/, February 25, 2008.

13. International Nuclear Energy Research Initiative, 2006 Annual Report. DOE/NE-131. Washington, DC: United States Department of Energy, 2007. p. 113.

14. Parma EJ, Vernon ME, Gelbard F, Moore RC, Stone HBJ, Pickard PS. Modeling the Sulfuric Acid Decomposition Section for Hydrogen Production. Proc, 2007 Int Topical Mtg on Safety and Technol of Nucl Hydrogen Prodn, Control, & Mgmt, Boston, MA, Jun 24-28, 2007: 154-160.

15. Ginosar DM, Glenn AW, Petkovic LM, Burch KC. Stability of supported platinum sulfuric acid decomposition catalysts for use in thermochemical water splitting cycles. Int J Hydrogen Energy 2007;32(4):482-488.

16. Ginosar DM, Rollins HW, Petkovic LM, Burch KC, Rush MJ. High-temperature sulfuric acid decomposition over complex metal oxide catalysts. Int J Hydrogen Energy 2008 (submitted for publication).

17. Mathias PM. General Atomics and Sandia National Laboratories; Modeling the Sulfur-Iodine Cycle; Aspen Plus™ Building Blocks and Simulation Models. Final Report from Aspen Technology, Inc. to General Atomics, Oct 24 2002.

18. Brown LC et al. High Efficiency Generation of Hydrogen Fuels Using Nuclear Power. Final Technical Report for the period August 1, 1999 through September 30, 2002, from General Atomics Corp. to US DOE, GA–A24285, Jun 2003, Appendix C.

19. Gmitro JI, Vermeulen T. Vapor-Liquid Equilibrium for Aqueous Sulfuric Acid. AIChE J 1964;10:740.

20. Kim SH, Roth M. Enthalpies of Dilution and Excess Molar Enthalpies of an Aqueous Solution of Sulfuric Acid. J Chem Eng Data 2001;46:138-143.

21. Fasullo OT. Sulfuric Acid: Use and Handling. New York: McGraw-Hill, 1965.

22. Wüster G, p, v, T – und Dampfdruckmessungen zur Bestimmung Thermodynamischer Eigenschaften Starker Elektrolyte bei Erhöhtem Druck. doctoral dissertation, RWTH-Aachen 1979.

23. Verfondern K (ed.). Nuclear Energy for Hydrogen Production. Jülich, Germany: Forschungszentrum Jülich GmbH, 2007.

24. Wang P, Anderko A, Springer RD, Young RD. Modeling phase equilibria and speciation in mixed-solvent electrolyte systems: II. Liquid–liquid equilibria and properties of associating electrolyte solutions J Molec Liquids 2006;125:37-44.

25. Miles FD, Fenton J. The solubility of sulfur dioxide in sulfuric acid. J Chem Soc 1920;117:59-61.

26. Kuznetsov DA. Study of the equilibrium pressures of sulfur dioxide over water and aqueous solutions of sulfuric acid (transl.). Zh Khim Prom (USSR.) 1941;18(22):3-7.

27. Miles FD, Carson T. Solubility of sulfur dioxide in fuming sulfuric acid. J Chem Soc 1946:786-90.

28.  Maass CE, Maass O. Sulfur dioxide and its aqueous solutions. I. Analytical methods, vapor density and vapor pressure of sulfur dioxide. Vapor pressure and concentrations of the solutions. J Am Chem Soc 1928;50(5):1352-1368.

29.  Spall BC. Phase equilibriums in the system sulfur dioxide-water from 25-300°. Can J Chem Engr 1963;41:79-83.

30.  van Berkum JG, Diepen GAM. Phase equilibriums in sulfur dioxide + water:  the sulfur dioxide gas hydrate, two liquid phases, and the gas phase in the temperature range 273 to 400 K and at pressures up to 400 MPa. J Chem Thermodynamics 1979;11:317-334.

31.  Staser J, Ramasamy RP, Sivasubramanian P, Weidner JW. Effect of Water on the Electrochemical Oxidation of Gas-Phase $SO_2$ in a PEM Electrolyzer for $H_2$ Production. Electrochem Solid-State Lett 2007;10:E17-E19.

32.  Areva NP. Olkiluoto 3, EPR – facts and figures. http://www.ol3.areva-np.com/project/facts.htm. May 29, 2008.

33.  Summers WA. Centralized Hydrogen Production from Nuclear Power: Infrastructure Analysis and Test-Case Design Study – Final Project Report, Phase B Test-Case Preconceptual Design, Savannah River National Laboratory Report No. WSRC-MS-2005-00693, Rev. 0, Apr 28 2006.

½O₂

Heat

$H_2SO_4 \xrightarrow[\text{(> 1073K)}]{> 800°C} \frac{1}{2}O_2 + SO_2 + H_2O$

Electric Energy

$H_2SO_4$

$SO_2 + H_2O$

$H_2 + H_2SO_4 \xleftarrow[\text{(373K)}]{100°C} SO_2 + 2H_2O$

H₂O

H₂
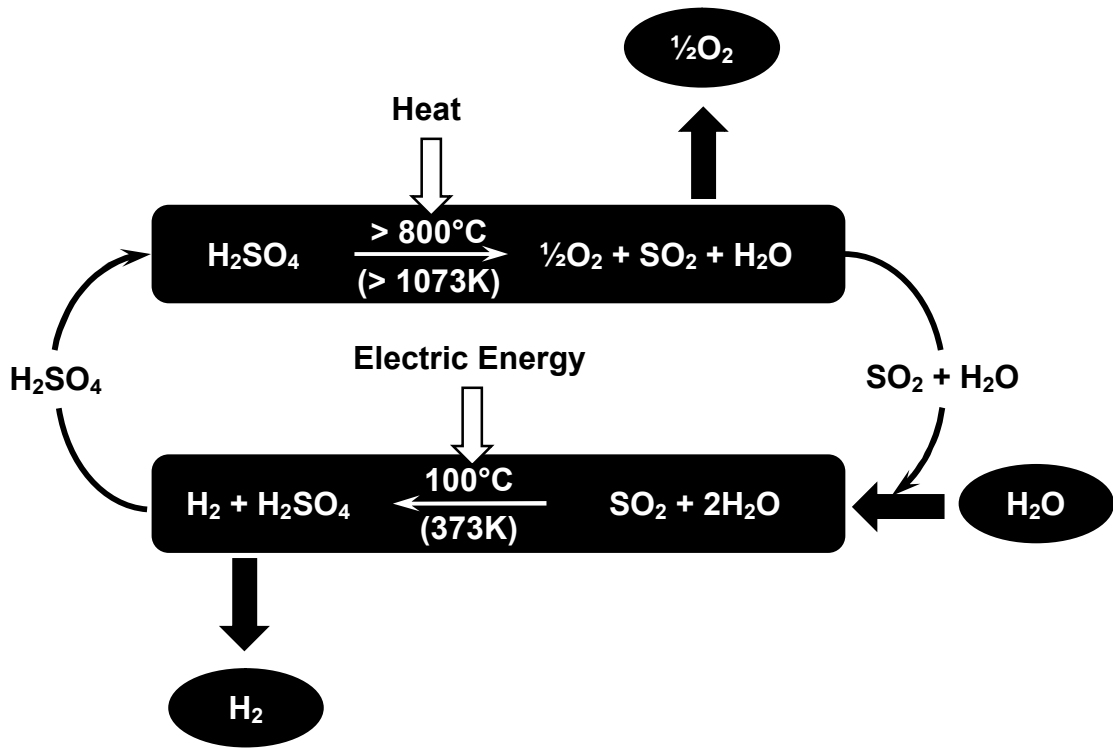
Figure 1

The Hybrid Sulfur (HyS) cycle

Maximilian B. Gorensek

Anode

Cathode

$2 e^-$

$H_2SO_4(aq)$

(+)

(−)

$SO_3(aq) + H_2O(l) \rightarrow$
$H_2SO_4(aq)$

$2 H^+$

$H_2(g)$

$2 H^+ + 2 e^- \rightarrow H_2(g)$

$SO_2(aq) + H_2O(l) \rightarrow$
$SO_3(aq) + 2 H^+ + 2 e^-$

$SO_2(aq), H_2O(l)$

Electrolyte Separator
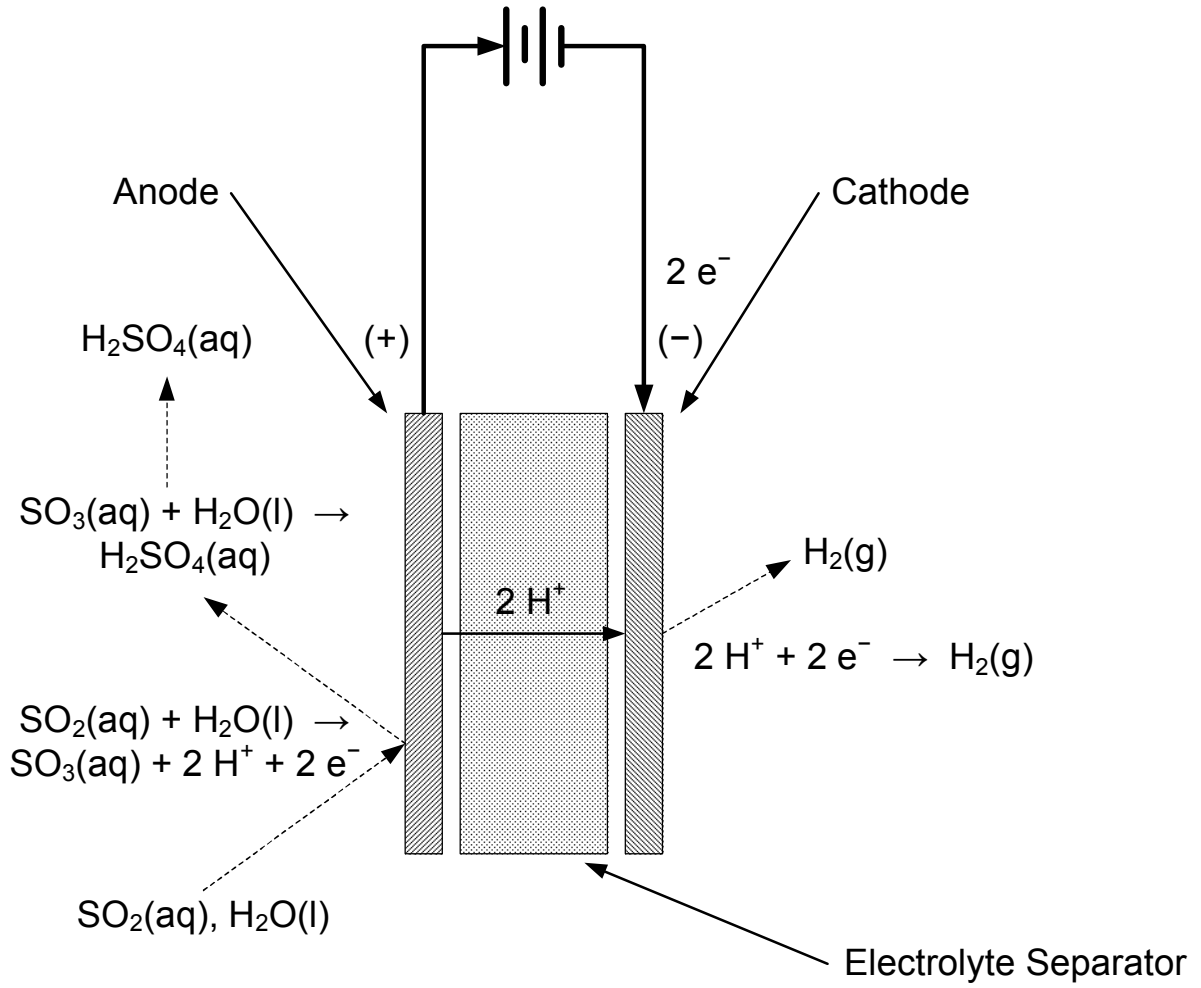
Figure 2

Schematic diagram of an SO$_2$-depolarized electrolyzer

Maximilian B. Gorensek

catalyst

High-
Temperature
Heat

$H_2SO_4$ in

Cool base

$SO_2$, $O_2$, $H_2O$ out
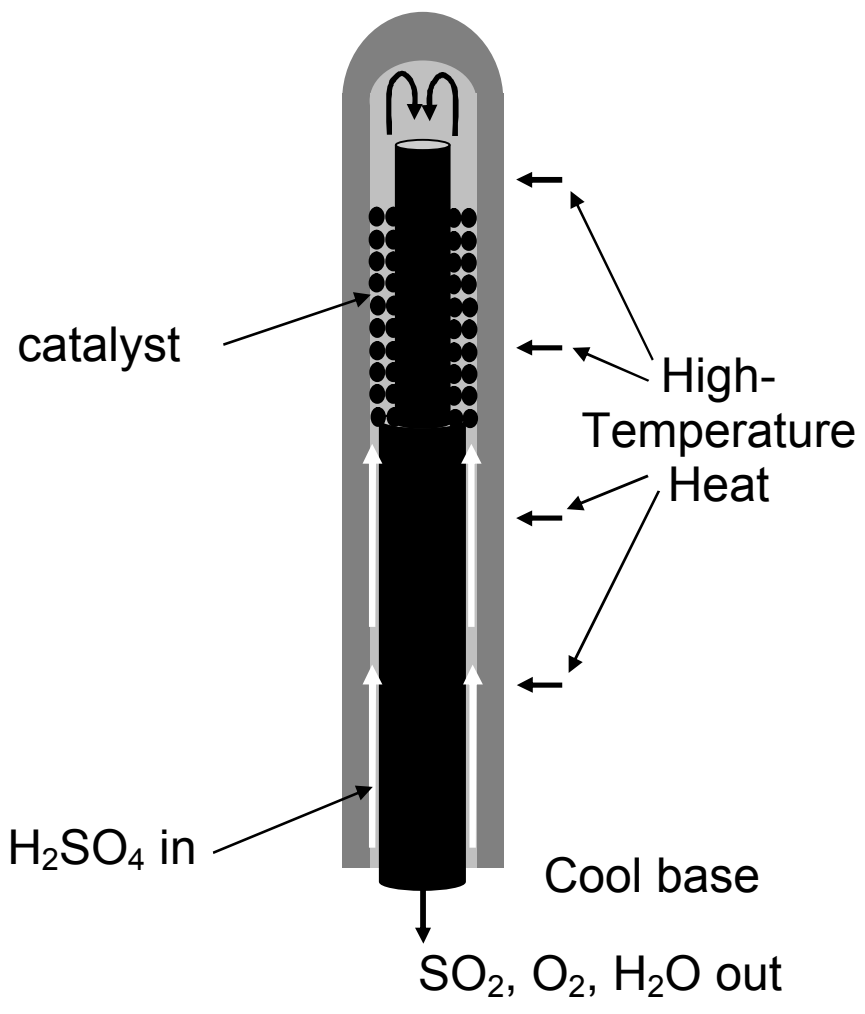
Figure 3

Schematic diagram of the SNL bayonet decomposition reactor

Maximilian B. Gorensek

# Vapor Pressure of Sulfuric Acid Solutions



Legend:
- ◆ 280 C
- ■ 300 C
- ▲ 340 C
- ▲ 400 C
- ◆ 440 C

Y-axis: Vapor Pressure (bar)

X-axis: Weight% Sulfuric Acid
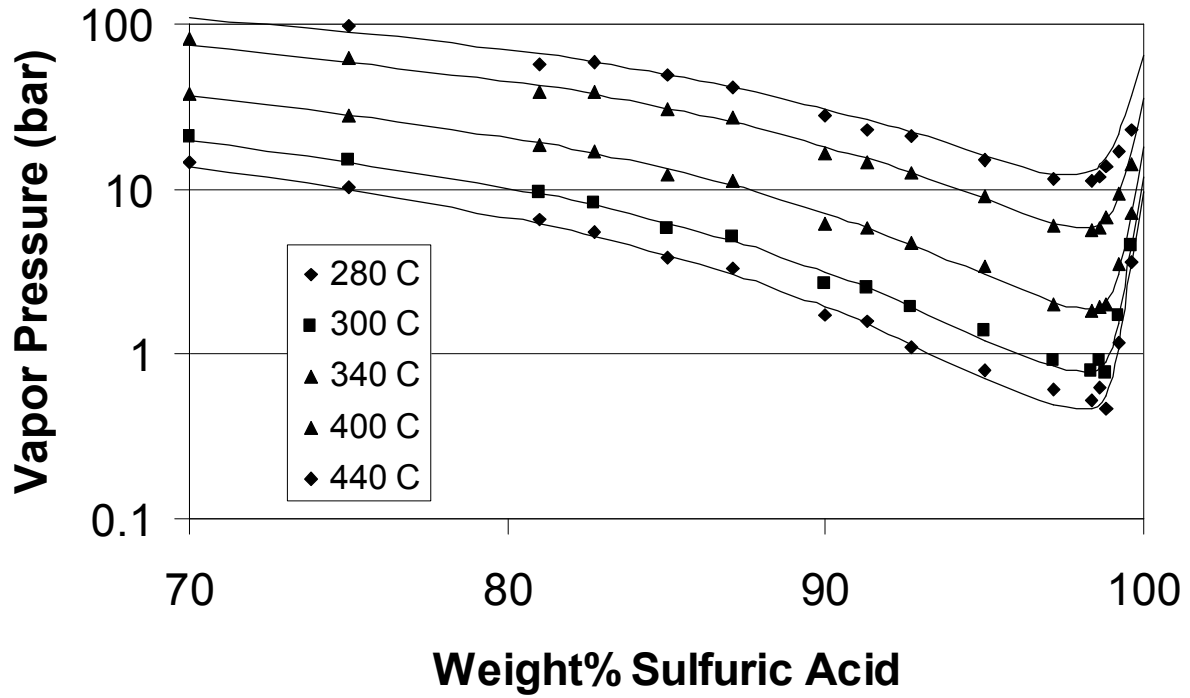
Figure 4

Vapor pressure of sulfuric acid solutions at high temperature – comparison of Mathias model with data of Wüster

Maximilian B. Gorensek

**Annulus**

Preheat — HTR1 — Q=101.17

Vaporize — HTR2 — Q=512.42

HTR3 — Q=21.87

Superheat — HTR4 — Q=124.86

Decompose — RXTR — Q=233.59

Stream 1: 120.00 / 76.0
Stream 2: 270.00 / 76.0
Stream 3: 552.65 / 76.0
Stream 4: 562.65 / 76.0
Stream 5: 675.00 / 76.0
Stream 6: 870.00 / 76.0

Cool — CLR1 — Q=-236.26

**Center**

Stream 7: 504.93 / 76.0
CLR2 — Q=-15.11
Stream 8: 494.93 / 76.0
Condense — CLR3 — Q=-353.62
Stream 9: 270.00 / 76.0
CLR4 — Q=-19.62
Stream 10: 255.00 / 76.0
DMY — Q=0.00
Stream 11: 255.00 / 76.0

Legend:
Temperature (C)
Pressure (bar)
Q  Duty (MW)

Figure 5

Aspen Plus™ high temperature decomposition reactor pinch analysis set-up flowsheet

Maximilian B. Gorensek
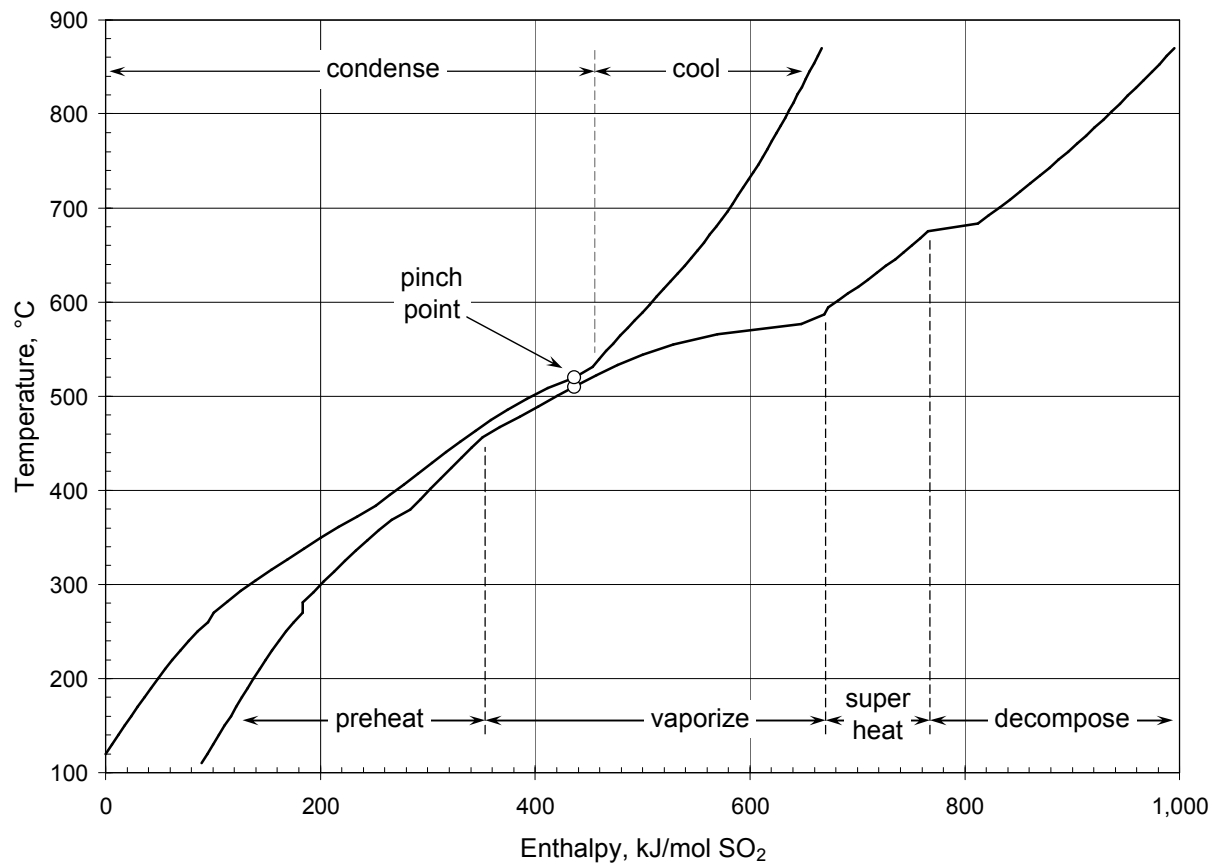
Figure 6

Bayonet Reactor heating and cooling curves – 80% $H_2SO_4$ feed, 86-bar pressure, 870 °C (1143 K) peak process temperature, 675 °C (948 K) catalyst bed inlet temperature

Maximilian B. Gorensek
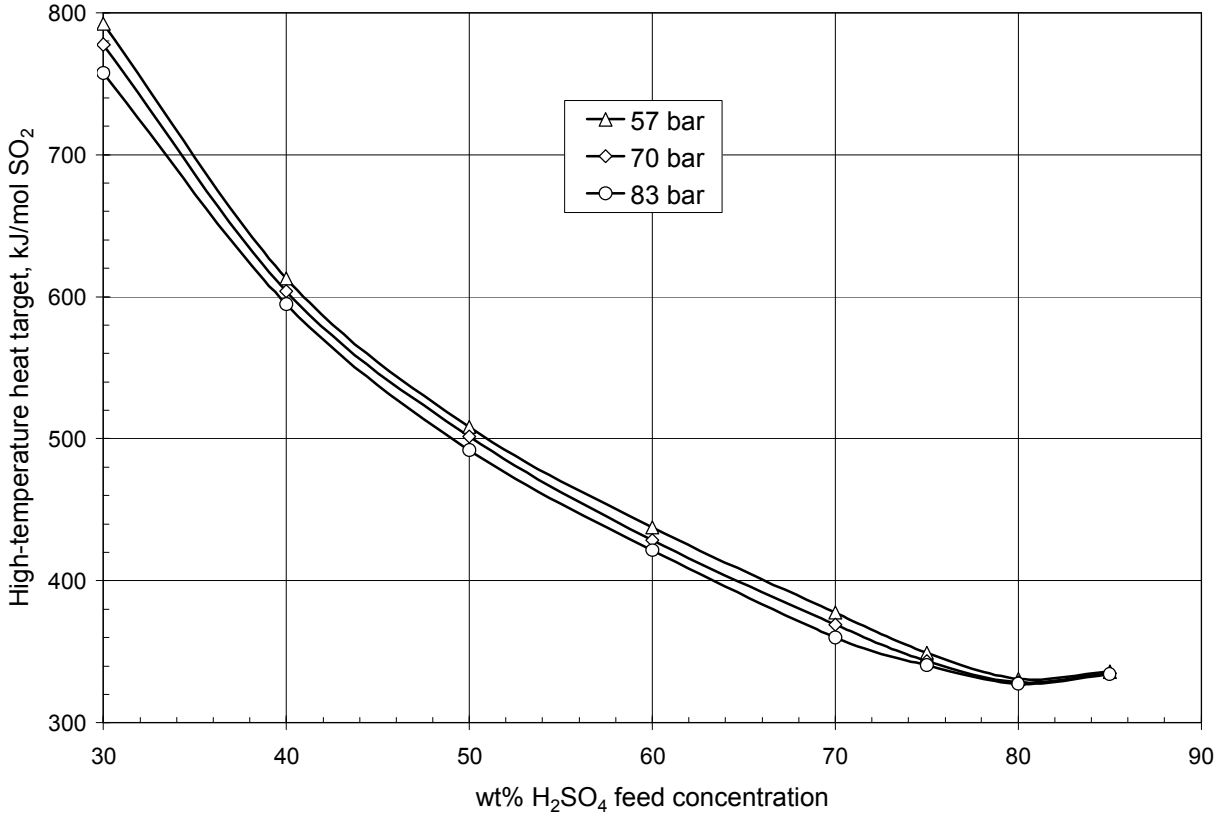
Figure 7

High-temperature heat requirement for $H_2SO_4$ decomposition as a function of feed concentration (30 to 85%) at three different pressures, 870 °C (1143 K) peak process temperature, 675 °C (948 K) catalyst bed inlet temperature

Maximilian B. Gorensek
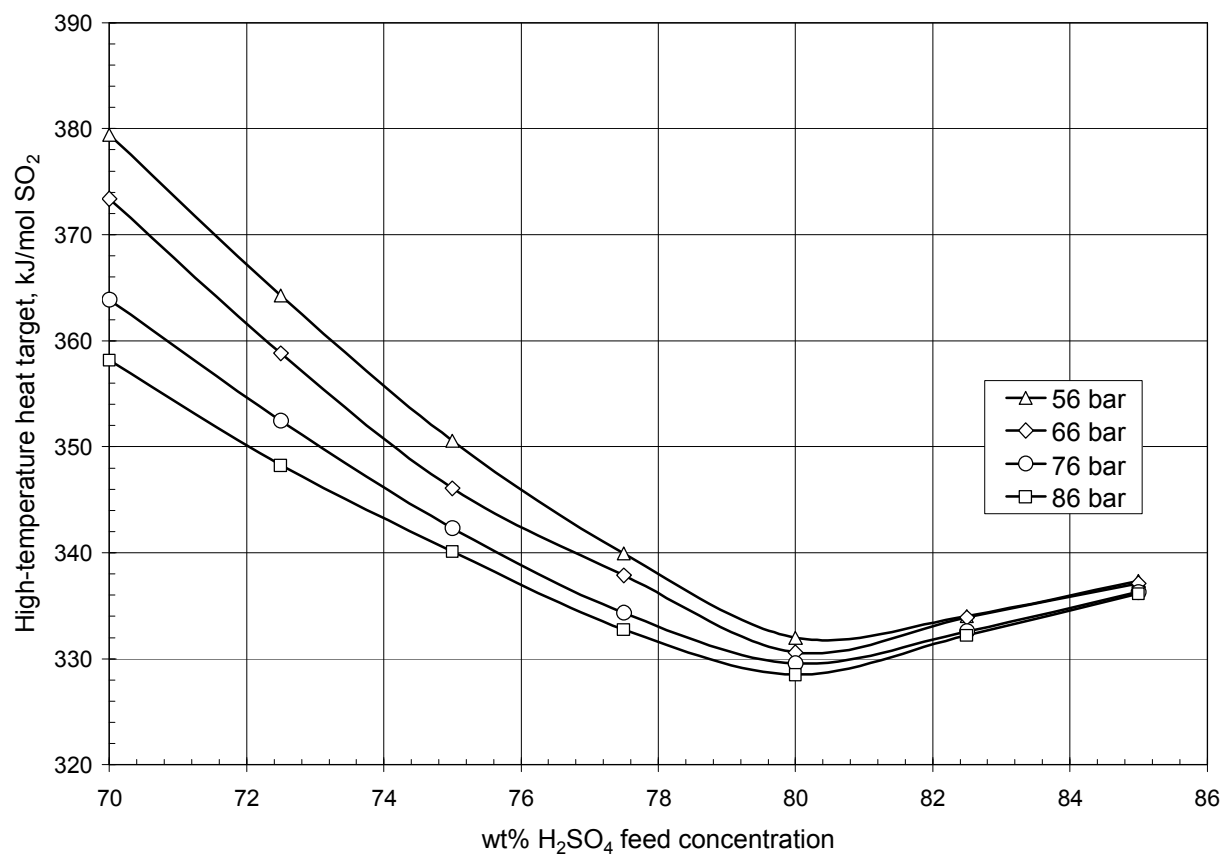
Figure 8

High-temperature heat requirement for $H_2SO_4$ decomposition as a function of feed concentration (70 to 85%) at four different pressures, 870 °C (1143 K) peak process temperature, 675 °C (948 K) catalyst bed inlet temperature

Maximilian B. Gorensek
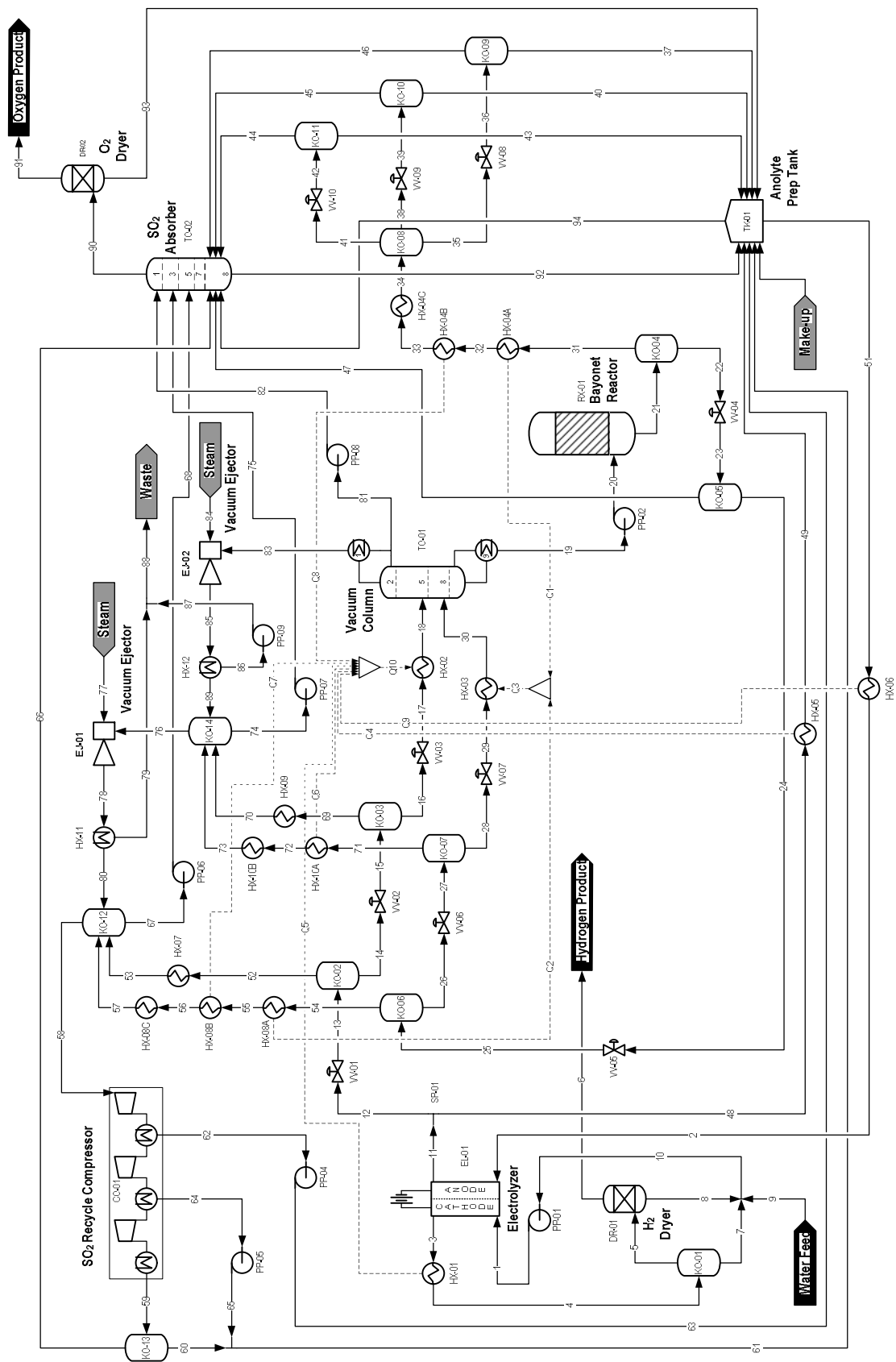
Figure 9

Hybrid Sulfur flowsheet using a PEM SDE and a bayonet decomposition reactor

Maximilian B. Gorensek
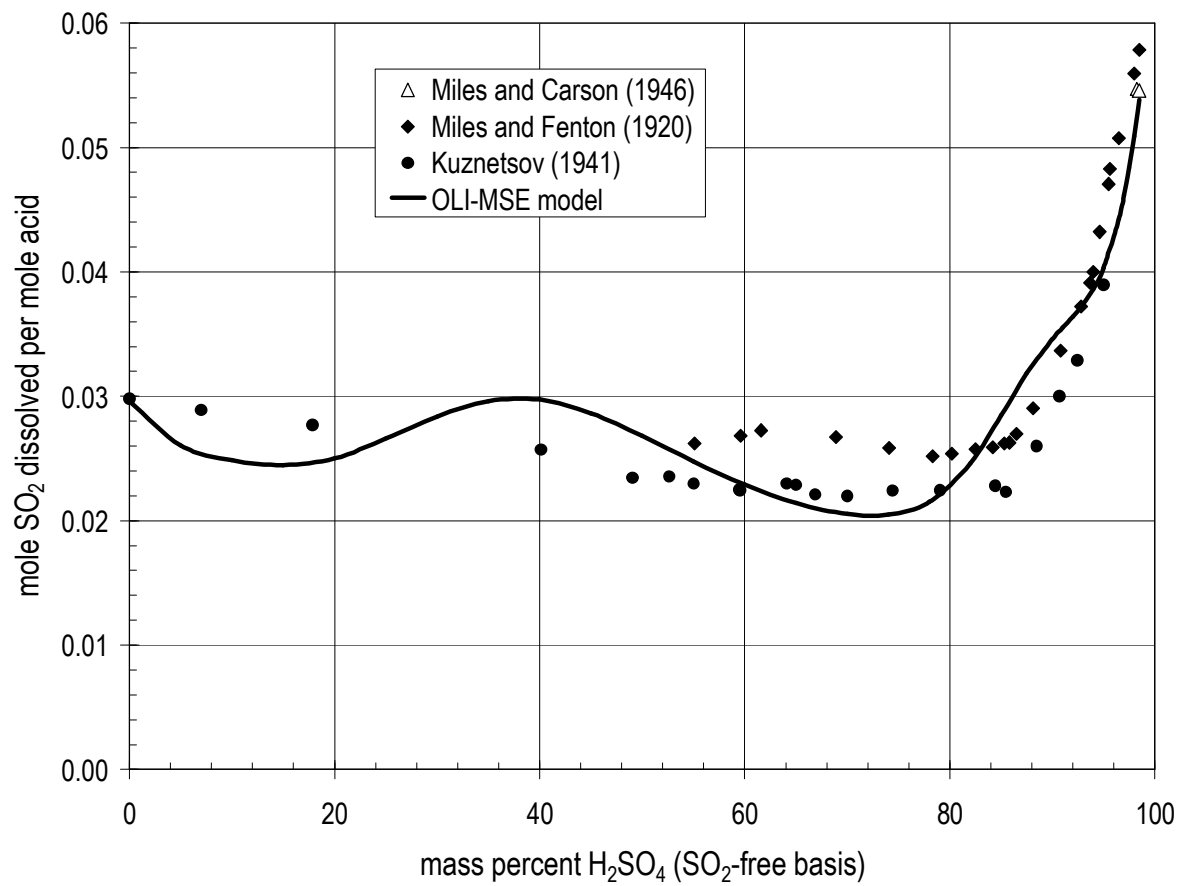
Figure 10

Solubility of $SO_2$ in sulfuric acid at 1.013-bar partial pressure – comparison of OLI MSE model with data of Miles and Carson, Kuznetsov, and Miles and Fenton

Maximilian B. Gorensek
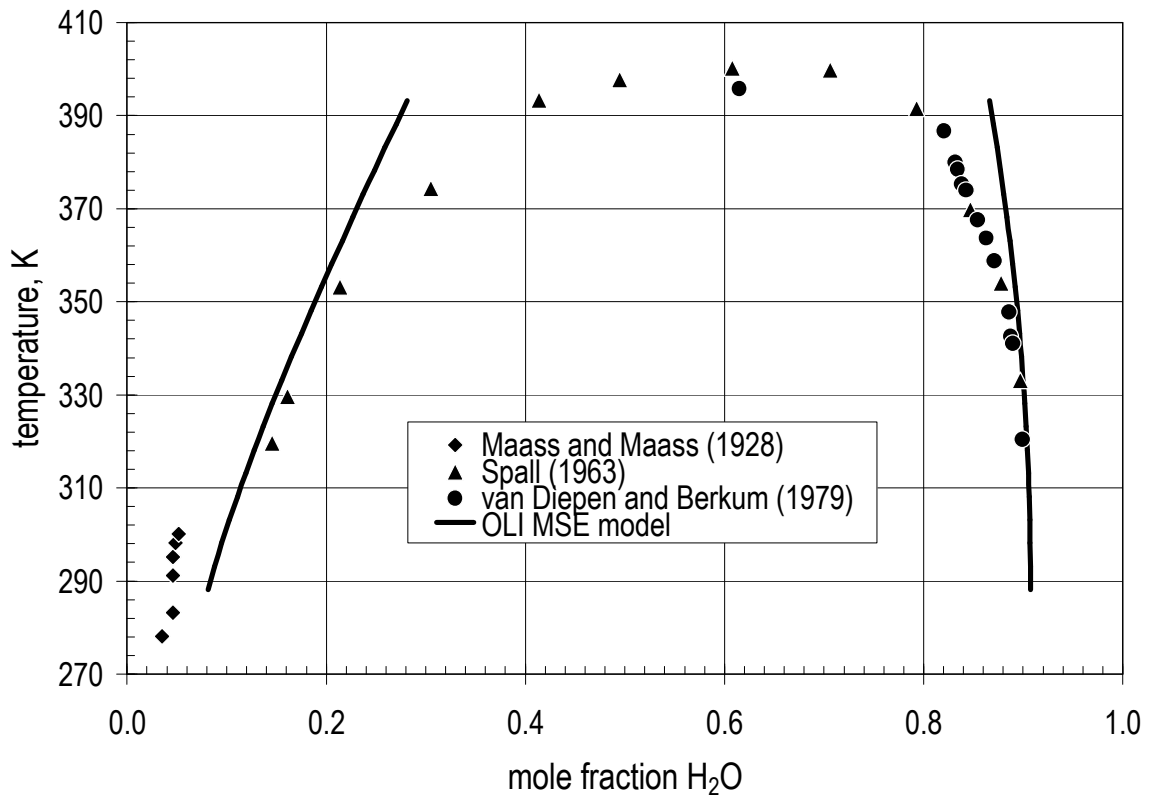
Figure 11

Liquid-liquid phase equilibrium in the $SO_2$-$H_2O$ system – comparison of OLI MSE model with data of Maass and Maass, Spall, and van Diepen and Berkum

Maximilian B. Gorensek

Table 1

Energy requirement allowances for HyS process

| | BWR/PWR Nuclear Power Plant | HTGR Nuclear Power Plant |
|---|---|---|
| Thermal-to-electric conversion efficiency, % | 33 | 45 |
| Water electrolysis efficiency (LHV), % | 68 | 68 |
| Nuclear-electrolysis plant efficiency (LHV), % | 22.4 | 30.6 |
| Thermal energy requirement, kJ/mol $H_2$ | 1,080 | 791 |
| HyS SDE cell voltage, V | -0.6 | -0.6 |
| Electricity demand, $kJ_e$/mol $H_2$ | 116 | 116 |
| Thermal equivalent of electricity, $kJ_{th}$/mol $H_2$ | 352 | 258 |
| Heat available for HyS high-temperature $H_2SO_4$ decomposition, kJ/mol $H_2$ | | |
|    For same efficiency as water electrolysis | 728 | 533 |
|    + 10% efficiency over water electrolysis | 630 | 461 |
|    + 25% efficiency over water electrolysis | 512 | 375 |
|    + 33% efficiency over water electrolysis | 460 | 337 |
|    + 50% efficiency over water electrolysis | 368 | 269 |

Table 2

Hybrid Sulfur flowsheet stream table

| Stream ID | Molar flow rates, kmol/sec | | | | | | Temperature, °C | K | Pressure, bar | Phase |
|---|---|---|---|---|---|---|---|---|---|---|
| | $H_2O$ | $H_2SO_4$ | $SO_2$ | $O_2$ | $H_2$ | Total | °C | K | bar | |
| 1 | 10 | 0 | 0 | 0 | 0.00235 | 10.0024 | 73.20 | 346.35 | 21 | L |
| 2 | 27.4794 | 3.88405 | 2.5 | 0.00527 | 0 | 37.7528 | 78.77 | 351.92 | 21 | L |
| 3 | 9 | 0 | 0 | 0 | 1.00235 | 10.0024 | 100.00 | 373.15 | 20 | L + V |
| 4 | 9 | 0 | 0 | 0 | 1.00235 | 10.0024 | 76.96 | 350.11 | 20 | L + V |
| 5 | 0.02185 | 0 | 0 | 0 | 1.00004 | 1.02189 | 76.96 | 350.11 | 20 | V |
| 6 | 0 | 0 | 0 | 0 | 1.00004 | 1.00004 | 40.00 | 313.15 | 20 | V |
| 7 | 8.97815 | 0 | 0 | 0 | 0.00231 | 8.98046 | 76.96 | 350.11 | 20 | L |
| 8 | 0.02185 | 0 | 0 | 0 | 0 | 0.02185 | 40.00 | 313.15 | 20 | L |
| 9 | 1 | 0 | 0 | 0 | 0 | 1 | 40.00 | 313.15 | 20 | L |
| 10 | 10 | 0 | 0 | 0 | 0.00231 | 10.0023 | 73.19 | 346.34 | 20 | L |
| 11 | 26.4794 | 4.88405 | 1.5 | 0.00527 | 0 | 37.7528 | 100.00 | 373.15 | 20 | L + V |
| 12 | 5.42394 | 1.00043 | 0.30725 | 0.00108 | 0 | 7.73314 | 100.00 | 373.15 | 20 | L + V |
| 13 | 5.42394 | 1.00043 | 0.30725 | 0.00108 | 0 | 7.73314 | 84.08 | 357.23 | 1.01325 | L + V |
| 14 | 5.33174 | 1.00043 | 0.02004 | 3.9E-07 | 0 | 7.35265 | 84.08 | 357.23 | 1.01325 | L |
| 15 | 5.33174 | 1.00043 | 0.02004 | 3.9E-07 | 0 | 7.35265 | 80.38 | 353.53 | 0.30198 | L + V |
| 16 | 5.29406 | 1.00043 | 0.00263 | 2.9E-10 | 0 | 7.29756 | 80.38 | 353.53 | 0.30198 | L |
| 17 | 5.29406 | 1.00043 | 0.00263 | 2.9E-10 | 0 | 7.29756 | 66.96 | 340.11 | 0.11 | L + V |
| 18 | 5.29406 | 1.00043 | 0.00263 | 2.9E-10 | 0 | 7.29756 | 94.41 | 367.56 | 0.11 | L + V |
| 19 | 3.7702 | 2.07782 | 6.7E-12 | 2E-21 | 0 | 7.92584 | 122.87 | 396.02 | 0.13 | L |
| 20 | 3.7702 | 2.07782 | 6.7E-12 | 0 | 0 | 7.92584 | 123.63 | 396.78 | 86 | L |
| 21 | 4.77063 | 1.07739 | 1.00043 | 0.50021 | 0 | 8.42605 | 254.70 | 527.85 | 86 | L + V |
| 22 | 4.30695 | 1.07739 | 0.23587 | 0.00844 | 0 | 6.70604 | 254.70 | 527.85 | 86 | L |
| 23 | 4.30695 | 1.07739 | 0.23587 | 0.00844 | 0 | 6.70604 | 233.42 | 506.57 | 21 | L + V |
| 24 | 4.03002 | 1.07739 | 0.04733 | 8.9E-05 | 0 | 6.23222 | 233.42 | 506.57 | 21 | L |
| 25 | 4.03002 | 1.07739 | 0.04733 | 8.9E-05 | 0 | 6.23222 | 147.33 | 420.48 | 1.01325 | L + V |
| 26 | 3.13019 | 1.07739 | 0.00035 | 1.4E-08 | 0 | 5.28532 | 147.33 | 420.48 | 1.01325 | L |
| 27 | 3.13019 | 1.07739 | 0.00035 | 1.4E-08 | 0 | 5.28532 | 118.57 | 391.72 | 0.30198 | L + V |
| 28 | 2.87261 | 1.07739 | 3.7E-06 | 2.4E-12 | 0 | 5.02739 | 118.57 | 391.72 | 0.30198 | L |
| 29 | 2.87261 | 1.07739 | 3.7E-06 | 2.4E-12 | 0 | 5.02739 | 100.50 | 373.65 | 0.13 | L + V |
| 30 | 2.87261 | 1.07739 | 3.7E-06 | 2.4E-12 | 0 | 5.02739 | 114.62 | 387.77 | 0.13 | L + V |
| 31 | 0.46368 | 5.5E-06 | 0.76455 | 0.49177 | 0 | 1.72001 | 254.70 | 527.85 | 86 | V |
| 32 | 0.46368 | 5.5E-06 | 0.76455 | 0.49177 | 0 | 1.72002 | 110.50 | 383.65 | 86 | L + V |
| 33 | 0.46368 | 5.5E-06 | 0.76455 | 0.49177 | 0 | 1.72002 | 76.96 | 350.11 | 86 | L + V |
| 34 | 0.46368 | 5.5E-06 | 0.76455 | 0.49177 | 0 | 1.72002 | 40.00 | 313.15 | 86 | L + V |
| 35 | 0.08967 | 1.8E-07 | 0.65507 | 0.00123 | 0 | 0.74597 | 40.00 | 313.15 | 86 | L |
| 36 | 0.08967 | 1.8E-07 | 0.65507 | 0.00123 | 0 | 0.74597 | 41.78 | 314.93 | 21 | L + V |
| 37 | 0.08966 | 1.8E-07 | 0.65459 | 0.00025 | 0 | 0.74451 | 41.78 | 314.93 | 21 | L |

| | | | | | | | | | | |
|---|---|---|---|---|---|---|---|---|---|---|
| 38 | 0.37282 | 5.3E-06 | 0.03946 | 0.00066 | 0 | 0.41296 | 40.00 | 313.15 | 86 | L |
| 39 | 0.37282 | 5.3E-06 | 0.03946 | 0.00066 | 0 | 0.41296 | 40.99 | 314.14 | 21 | L + V |
| 40 | 0.37282 | 5.3E-06 | 0.03922 | 0.00014 | 0 | 0.41218 | 40.99 | 314.14 | 21 | L |
| 41 | 0.00119 | 0 | 0.07002 | 0.48988 | 0 | 0.56109 | 40.00 | 313.15 | 86 | V |
| 42 | 0.00119 | 0 | 0.07002 | 0.48988 | 0 | 0.56109 | 15.50 | 288.65 | 21 | L + V |
| 43 | 0.0006 | 0 | 4.7E-05 | 3.8E-07 | 0 | 0.00065 | 15.50 | 288.65 | 21 | L |
| 44 | 0.00059 | 0 | 0.06997 | 0.48988 | 0 | 0.56044 | 15.50 | 288.65 | 21 | V |
| 45 | 3.5E-06 | 4.3E-26 | 0.00025 | 0.00052 | 0 | 0.00077 | 40.99 | 314.14 | 21 | V |
| 46 | 6.9E-06 | 1E-25 | 0.00048 | 0.00098 | 0 | 0.00146 | 41.78 | 314.93 | 21 | V |
| 47 | 0.27692 | 1.3E-06 | 0.18854 | 0.00835 | 0 | 0.47382 | 233.42 | 506.57 | 21 | V |
| 48 | 21.0554 | 3.88362 | 1.19275 | 0.00419 | 0 | 30.0196 | 100.00 | 373.15 | 20 | L + V |
| 49 | 21.0554 | 3.88362 | 1.19275 | 0.00419 | 0 | 30.0196 | 80.00 | 353.15 | 20 | L |
| 50 | 21.0554 | 3.88362 | 1.19275 | 0.00419 | 0 | 30.0196 | 80.01 | 353.16 | 21 | L |
| 51 | 27.4794 | 3.88405 | 2.5 | 0.00524 | 0 | 37.7527 | 84.71 | 357.86 | 21 | L |
| 52 | 0.0922 | 2E-11 | 0.28721 | 0.00108 | 0 | 0.38049 | 84.08 | 357.23 | 1.01325 | V |
| 53 | 0.0922 | 2E-11 | 0.28721 | 0.00108 | 0 | 0.38049 | 40.00 | 313.15 | 1.01325 | L + V |
| 54 | 0.89983 | 6.6E-07 | 0.04698 | 8.9E-05 | 0 | 0.9469 | 147.33 | 420.48 | 1.01325 | V |
| 55 | 0.89983 | 6.6E-07 | 0.04698 | 8.9E-05 | 0 | 0.9469 | 110.50 | 383.65 | 1.01325 | L + V |
| 56 | 0.89983 | 6.6E-07 | 0.04698 | 8.9E-05 | 0 | 0.9469 | 76.96 | 350.11 | 1.01325 | L + V |
| 57 | 0.89983 | 6.6E-07 | 0.04698 | 8.9E-05 | 0 | 0.9469 | 40.00 | 313.15 | 1.01325 | L + V |
| 58 | 0.02674 | 2.3E-24 | 0.33759 | 0.00117 | 0 | 0.3655 | 40.00 | 313.15 | 1.01325 | V |
| 59 | 1.9E-05 | 0 | 0.00541 | 0.00116 | 0 | 0.00659 | 40.00 | 313.15 | 21 | L + V |
| 60 | 1.9E-05 | 0 | 0.0048 | 1.2E-06 | 0 | 0.00482 | 40.00 | 313.15 | 21 | L |
| 61 | 0.00936 | 0 | 0.33626 | 1E-05 | 0 | 0.34562 | 41.20 | 314.35 | 21 | L |
| 62 | 0.01738 | 0 | 0.00073 | 3.5E-09 | 0 | 0.01811 | 40.00 | 313.15 | 2.78324 | L |
| 63 | 0.01738 | 0 | 0.00073 | 3.5E-09 | 0 | 0.01811 | 41.11 | 314.26 | 21 | L |
| 64 | 0.00934 | 0 | 0.33146 | 9.2E-06 | 0 | 0.3408 | 40.00 | 313.15 | 7.64513 | L |
| 65 | 0.00934 | 0 | 0.33146 | 9.2E-06 | 0 | 0.3408 | 41.22 | 314.37 | 21 | L |
| 66 | 3.2E-07 | 0 | 0.00061 | 0.00116 | 0 | 0.00177 | 40.00 | 313.15 | 21 | V |
| 67 | 0.96665 | 6.6E-07 | 0.01365 | 6.1E-08 | 0 | 0.9803 | 40.00 | 313.15 | 1.01325 | L |
| 68 | 0.96665 | 6.6E-07 | 0.01365 | 6.1E-08 | 0 | 0.9803 | 40.31 | 313.46 | 21 | L |
| 69 | 0.03768 | 6.4E-12 | 0.01741 | 3.9E-07 | 0 | 0.0551 | 80.38 | 353.53 | 0.30198 | V |
| 70 | 0.03768 | 6.4E-12 | 0.01741 | 3.9E-07 | 0 | 0.0551 | 40.00 | 313.15 | 0.30198 | L + V |
| 71 | 0.25758 | 1E-07 | 0.00035 | 1.4E-08 | 0 | 0.25793 | 118.57 | 391.72 | 0.30198 | V |
| 72 | 0.25758 | 1E-07 | 0.00035 | 1.4E-08 | 0 | 0.25793 | 76.96 | 350.11 | 0.30198 | L + V |
| 73 | 0.25758 | 1E-07 | 0.00035 | 1.4E-08 | 0 | 0.25793 | 40.00 | 313.15 | 0.30198 | L |
| 74 | 0.28961 | 1E-07 | 0.00106 | 2.8E-11 | 0 | 0.29067 | 40.61 | 313.76 | 0.30198 | L |
| 75 | 0.28961 | 1E-07 | 0.00106 | 2.8E-11 | 0 | 0.29067 | 41.14 | 314.29 | 21 | L |
| 76 | 0.0059 | 1.2E-25 | 0.01745 | 4.1E-07 | 0 | 0.02335 | 40.61 | 313.76 | 0.30198 | V |
| 77 | 0.02335 | 0 | 0 | 0 | 0 | 0.02335 | 169.99 | 443.14 | 7.91 | L + V |
| 78 | 0.02925 | 0 | 0.01745 | 4.1E-07 | 0 | 0.0467 | 93.77 | 366.92 | 1.01325 | V |
| 79 | 0.0279 | 0 | 0.0004 | 1.2E-11 | 0 | 0.0283 | 40.00 | 313.15 | 1.01325 | L |

| | | | | | | | | | | |
|---|---|---|---|---|---|---|---|---|---|---|
| 80 | 0.00135 | 0 | 0.01706 | 4.1E-07 | 0 | 0.0184 | 40.00 | 313.15 | 1.01325 | V |
| 81 | 4.39285 | 6.9E-35 | 0.00185 | 4.9E-13 | 0 | 4.3947 | 40.02 | 313.17 | 0.09 | L |
| 82 | 4.39285 | 0 | 0.00185 | 4.9E-13 | 0 | 4.3947 | 40.21 | 313.36 | 21 | L |
| 83 | 0.00361 | 5.2E-35 | 0.00079 | 3E-10 | 0 | 0.0044 | 40.02 | 313.17 | 0.09 | V |
| 84 | 0.0044 | 0 | 0 | 0 | 0 | 0.0044 | 169.99 | 443.14 | 7.91 | L + V |
| 85 | 0.00801 | 0 | 0.00079 | 3E-10 | 0 | 0.0088 | 95.05 | 368.20 | 0.30198 | V |
| 86 | 0.00777 | 0 | 2.9E-05 | 1.3E-14 | 0 | 0.0078 | 40.00 | 313.15 | 0.30198 | L |
| 87 | 0.00777 | 0 | 2.9E-05 | 1.3E-14 | 0 | 0.0078 | 40.04 | 313.19 | 1.01325 | L |
| 88 | 0.03567 | 0 | 0.00042 | 1.2E-11 | 0 | 0.03609 | 40.03 | 313.18 | 1.01325 | L |
| 89 | 0.00025 | 0 | 0.00076 | 3E-10 | 0 | 0.001 | 40.00 | 313.15 | 0.30198 | V |
| 90 | 0.00228 | 1.4E-34 | 0.00413 | 0.50024 | 0 | 0.50665 | 41.12 | 314.27 | 21 | V |
| 91 | 0 | 0 | 0 | 0.50024 | 0 | 0.50024 | 40.00 | 313.15 | 21 | V |
| 92 | 5.92438 | 2.1E-06 | 0.27327 | 0.00116 | 0 | 6.19882 | 82.33 | 355.48 | 21 | L |
| 93 | 0.00228 | 0 | 0.00413 | 0 | 0 | 0.00641 | 40.00 | 313.15 | 21 | L |
| 94 | 2.9E-05 | 7.6E-16 | 0.00098 | 0.00051 | 0 | 0.00152 | 84.71 | 357.86 | 21 | V |
| MAKE UP | 0.00749 | 0.00042 | 0 | 0 | 0 | 0.00834 | 40.00 | 313.15 | 21 | L |

Table 3

Hybrid Sulfur flowsheet heat exchangers

| Block ID | Duty, MW$_{th}$ | Temperature, °C (K) | | Heat Exchanged With: |
|---|---|---|---|---|
| | | Inlet | Outlet | |
| CO-01/Stage 1 Cooler | -2.290 | 138.02 (411.2) | 40.0 (313) | Cooling Water |
| CO-01/Stage 2 Cooler | -9.109 | 137.79 (410.9) | 40.0 (313) | Cooling Water |
| CO-01/Stage 3 Cooler | -0.132 | 143.76 (416.9) | 40.0 (313) | Cooling Water |
| DR-01 | -2.045 | 76.96 (350.1) | 40.0 (313) | Cooling Water |
| DR-02 | -0.197 | 41.12 (314.3) | 40.0 (313) | Cooling Water |
| HX-01 | -17.688 | 100.00 (373.0) | 76.96 (350.1) | HX-02 |
| HX-02 | 130.486 | 66.96 (340.1) | 94.41 (367.6) | HX-01, HX-04B, HX-05, HX-06, HX08B, HX-10A |
| HX-03 | 31.777 | 100.50 (373.7) | 114.62 (387.8) | HX-04A, HX-08A |
| HX-04A | -30.543 | 254.70 (527.9) | 110.50 (383.7) | HX-03 |
| HX-04B | -8.400 | 110.50 (383.7) | 76.96 (350.1) | HX-02 |
| HX-04C | -6.243 | 76.96 (350.1) | 40.0 (313) | Cooling Water |
| HX-05 | -47.903 | 100.00 (373.0) | 80.00 (353.0) | HX-02 |
| HX-06 | -18.686 | 84.71 (357.9) | 78.77 (351.9) | HX-02 |
| HX-07 | -3.702 | 84.08 (357.2) | 40.0 (313) | Cooling Water |
| HX-08A | -1.234 | 147.33 (420.5) | 110.50 (383.7) | HX-03 |
| HX-08B | -37.440 | 110.50 (383.7) | 76.96 (350.1) | HX-02 |
| HX-08C | -4.021 | 76.96 (350.1) | 40.0 (313) | Cooling Water |
| HX-09 | -1.476 | 80.38 (353.5) | 40.0 (313) | Cooling Water |
| HX-10A | -0.368 | 118.57 (391.7) | 76.96 (350.1) | HX-02 |
| HX-10B | -11.503 | 76.96 (350.1) | 40.0 (313) | Cooling Water |
| HX-11 | -1.310 | 93.77 (366.9) | 40.0 (313) | Cooling Water |
| HX-12 | -0.354 | 95.05 (368.2) | 40.0 (313) | Cooling Water |
| RX-01 | 340.280 | 123.63 (396.8) | 254.70 (527.9) | High-Temp. Source |
| TO-01 Reboiler | 75.482 | 102.74 (375.9) | 122.87 (396.0) | Low-Temp. Source |
| TO-01 Condenser | -210.542 | 44.80 (318.0) | 40.0 (313) | Cooling Water |

Table 4

Hybrid Sulfur flowsheet electrolyzers, pumps, and compressors

| Block ID | Work, $MW_e$ |
| --- | --- |
| EL-01 | 115.782 |
| CO-01/Stage 1 | 1.464 |
| CO-01/Stage 2 | 1.357 |
| CO-01/Stage 3 | 0.025 |
| PP-01 | 0.022 |
| PP-02 | 1.836 |
| PP-03 | 0.071 |
| PP-04 | 0.002 |
| PP-05 | 0.028 |
| PP-06 | 0.055 |
| PP-07 | 0.021 |
| PP-08 | 0.212 |
| PP-09 | 0.00003 |